Open clusters. III. Fundamental parameters of B stars in NGC 6087, NGC 6250, NGC 6383, and NGC 6530 B-type stars with circumstellar envelopes

Y. Aidelman, L. S. Cidale, J. Zorec, J. A. Panei

A&A 610, A30 (2018)
DOI: 10.1051/0004-6361/201730995

Astronomy & Astrophysics

Open clusters

III. Fundamental parameters of B stars in NGC 6087, NGC 6250, NGC 6383, and NGC 6530

B-type stars with circumstellar envelopes[⋆,⋆⋆]

Y. Aidelman[1,2,⋆⋆⋆], L. S. Cidale[1,2,⋆⋆⋆⋆], J. Zorec[3,4], and J. A. Panei[1,2,⋆⋆⋆⋆]

[1] Instituto de Astrofísica La Plata, CCT La Plata, CONICET-UNLP, Paseo del Bosque S/N, B1900FWA, La Plata, Argentina
e-mail: aidelman@fcaglp.unlp.edu.ar
[2] Departamento de Espectroscopía, Facultad de Ciencias Astronómicas y Geofísicas, Universidad Nacional de La Plata (UNLP), Paseo del Bosque S/N, B1900FWA, La Plata, Argentina
[3] Sorbonne Université, UPMC Univ. Paris 06, 934 UMR 7095-IAP, 75014 Paris, France
[4] CNRS, 934 UMR7095-IAP, Institut d'Astrophysique de Paris, 98 bis Bd. Arago, 75014 Paris, France

Received 17 April 2017 / Accepted 26 October 2017

ABSTRACT

Context. Stellar physical properties of star clusters are poorly known and the cluster parameters are often very uncertain.
Aims. Our goals are to perform a spectrophotometric study of the B star population in open clusters to derive accurate stellar parameters, search for the presence of circumstellar envelopes, and discuss the characteristics of these stars.
Methods. The BCD spectrophotometric system is a powerful method to obtain stellar fundamental parameters from direct measurements of the Balmer discontinuity. To this end, we wrote the interactive code MIDE3700. The BCD parameters can also be used to infer the main properties of open clusters: distance modulus, color excess, and age. Furthermore, we inspected the Balmer discontinuity to provide evidence for the presence of circumstellar disks and identify Be star candidates. We used an additional set of high-resolution spectra in the Hα region to confirm the Be nature of these stars.
Results. We provide $T_{\rm eff}$, log g, $M_{\rm v}$, $M_{\rm bol}$, and spectral types for a sample of 68 stars in the field of the open clusters NGC 6087, NGC 6250, NGC 6383, and NGC 6530, as well as the cluster distances, ages, and reddening. Then, based on a sample of 230 B stars in the direction of the 11 open clusters studied along this series of three papers, we report 6 new Be stars, 4 blue straggler candidates, and 15 B-type stars (called Bdd) with a double Balmer discontinuity, which indicates the presence of circumstellar envelopes. We discuss the distribution of the fraction of B, Be, and Bdd star cluster members per spectral subtype. The majority of the Be stars are dwarfs and present a maximum at the spectral type B2-B4 in young and intermediate-age open clusters (<40 Myr). Another maximum of Be stars is observed at the spectral type B6-B8 in open clusters older than 40 Myr, where the population of Bdd stars also becomes relevant. The Bdd stars seem to be in a passive emission phase.
Conclusions. Our results support previous statements that the Be phenomenon is present along the whole main sequence band and occurs in very different evolutionary states. We find clear evidence of an increase of stars with circumstellar envelopes with cluster age. The Be phenomenon reaches its maximum in clusters of intermediate age (10−40 Myr) and the number of B stars with circumstellar envelopes (Be plus Bdd stars) is also high for the older clusters (40−100 Myr).

Key words. open clusters and associations: individual: NGC 6087 – open clusters and associations: individual: NGC 6250 – open clusters and associations: individual: NGC 6383 – open clusters and associations: individual: NGC 6530 – stars: fundamental parameters – stars: emission-line, Be

1. Introduction

This is the third of a series of papers devoted to the spectroscopic study of a total of 230 B-type stars in the field of view of 11 open clusters. This study is based on the spectrophotometric BCD (Barbier-Chalonge-Divan) system, developed by Barbier & Chalonge (1939) and Chalonge & Divan (1973).

Our main goals were to derive accurate stellar parameters ($T_{\rm eff}$, log g, $M_{\rm v}$, $M_{\rm bol}$, and spectral types) of the B star population in open clusters and search for the presence of B stars with circumstellar envelopes. A secondary objective was to provide an improved set of cluster parameters and identify their star memberships.

Particularly, this work presents a spectrophotometric investigation of 68 B-type stars in the region of the galactic clusters NGC 6087, NGC 6250, NGC 6383, and NGC 6530. The results related to 7 other clusters were published by Aidelman et al. (2012, 2015, hereafter Paper I and Paper II, respectively). In addition, all of the information gathered in this series of papers allows us to analyze here the relative frequency of cluster star members per spectral subtypes and age and the distribution of stars with circumstellar envelopes in a $T_{\rm eff}$ − log g diagram, and

⋆ Observations taken at CASLEO, operating under agreement of CONICET and the Universities of La Plata, Córdoba, and San Juan, Argentina.
⋆⋆ Tables 1, 2, 9–16 are only available at the CDS via anonymous ftp to cdsarc.u-strasbg.fr (130.79.128.5) or via http://cdsarc.u-strasbg.fr/viz-bin/qcat?J/A+A/610/A30
⋆⋆⋆ Fellow of CONICET, Argentina.
⋆⋆⋆⋆ Member of the Carrera del Investigador Científico, CONICET, Argentina.

to discuss some characteristics of the peculiar group of Be stars. In Paper I, we introduced the BCD method as a tool to evaluate precise physical parameters of the stars in a cluster and cluster properties, in a fast and direct way, by measuring the Balmer discontinuity (BD). On the other hand, as the BCD parameters are not affected by interstellar absorption or circumstellar emission or absorption (Zorec & Briot 1991), the location of stars in the Hertzsprung-Russell (HR) diagram is more accurate than classical methods based on plain photometry, thus allowing for better determinations of cluster ages. Moreover, the BCD method also enables us to characterize each star in very crowded stellar regions with fundamental parameters that cannot be strongly perturbed by the light of the nearest objects, so that it is possible to discuss properly their cluster membership by taking color excesses and distance estimates, as in Paper II.

Another advantage of the study of the BD is that it allows us to recognize B stars with circumstellar envelopes since some B-type stars display a second component of the BD (called hereafter SBD; for more details, see Divan 1979; Zorec & Briot 1991; Cidale et al. 2001; Zorec et al. 2005; Cidale et al. 2007 and Paper I). The main BD, in absorption, occurs as in normal dwarf stars and is attributed to the central star. The SBD is situated at shorter wavelengths and is originated in an envelope with low pressure (Divan 1979). A SBD in absorption is often related to spectral line "shell" signatures, while a SBD in emission is generally accompanied by line emission features. We can then use the SBD, when is present, as a criterion to detect stars with circumstellar envelopes or disks. This is possible even though they do not exhibit clear signs of emission or shell-absorption features among the first attainable members of the Balmer lines, as a consequence of a late B spectral type or the low resolution of the available spectrophotometric spectra. Therefore, as a complement of this work, we present spectra of B stars in open clusters that exhibit a SBD and discuss the properties of this star population (see details in Sects. 5.2 and 5.3).

The paper is organized as follows: data acquisition and reduction procedure are given in Sect. 2. In Sect. 3 we briefly describe the BCD method and its application to our star sample. Spectrophotometric results on the cluster parameters (NGC 6087, NGC 6250, NGC 6383, and NGC 6530) and their memberships are given in Sect. 4. In Sect. 5 we analyze the relative frequency of B and Be stars per spectral subtypes and age, using data of the 11 open clusters studied. We discuss the derived stellar parameters and presence of circumstellar envelopes in late B-type stars. Our conclusions are summarized in Sect. 6.

2. Observations

Low-resolution spectra of additional 68 B-type stars in four open clusters were obtained in long slit mode during multiple observing runs between 2003 and 2013 with a Boller & Chivens spectrograph[1] attached to the *J. Sahade* 2.15 m telescope at the Complejo Astronómico El Leoncito (CASLEO), San Juan, Argentina. The log of observations is listed in Table 1 (available at the CDS). The spectra were taken with a Bausch and Lomb replica diffraction grating of 600 l mm^{-1} (#80, blazed at 4000 Å) and slit widths of 250 μm and 350 μm oriented along east-west. The slit widths were set to match an aperture on the sky of about 2.″3 and 3.″3, respectively, according to the average seeing at CASLEO.

Before 2011, we used a PM 512 CCD detector covering the spectral wavelength range of 3500−4700 Å. The rest of the observations were carried out with the CCD detector TEK 1024 that covered the wavelength interval 3500−5000 Å. The effective spectral resolutions are 4.53 Å and 2.93 Å every two pixels ($R \sim 900$, $R \sim 1400$), respectively. A comparison lamp of He-Ne-Ar was taken after each science stellar spectrum.

The observations were performed at the lowest possible zenith distance to minimize refraction effects due to the Earth's atmosphere and, thus, to avoid light losses as a function of wavelength. For an air mass of 1.5 the expected differential refraction effect between 4000 Å and 6000 Å is 1.″08[2]. This assures that the light loss is minimized. Each night we observed at least two flux standard stars (HR 3454, HR 5501, HR 7596, HR 4468, and HR 5694) to perform the spectral flux calibrations.

The reduction procedure (overscan, bias, trimming, and flat-field corrections) was carried out with the IRAF[3] software package (version 2.14.1) and all spectra were wavelength calibrated and corrected for atmospheric extinction. We used the atmospheric extinction coefficients published in CASLEO web page[4].

An addition set of high-resolution spectra ($R = 12\,600$) were taken with the echelle spectrograph REOSC in the spectral range 4225−6700 Å to seek the Hα emission in the B stars with a SBD. These observations were carried out only for some of the star members identified in the 11 studied Galactic clusters (see Table 2, available at the CDS). The instrumental configuration was a 400 l mm^{-1} grating (#580), 250 μm slit, and TK 1K CCD detector. A Th-Ar comparison lamp was used to apply the wavelength calibration.

3. Method

As was previously described in Papers I and II, we derived the fundamental parameters of open clusters and individual stars from low-resolution spectroscopic data with the BCD spectrophotometric method.

For each star of our sample we measured the BCD parameters: λ_1, D, and $\Phi_{\rm b}$ (or $\Phi_{\rm bb}$). The first two parameters describe the average spectral position and height of the BD, respectively. The third parameter is the color gradient that measures the slope of the Paschen continuum. Then using the BCD calibrations (see Paper I) we obtained the stellar fundamental parameters: spectral type, luminosity class, effective temperature ($T_{\rm eff}$), logarithm of surface gravity ($\log g$), absolute visual magnitude ($M_{\rm v}$), absolute bolometric magnitude ($M_{\rm bol}$), and intrinsic color gradient ($\Phi^0_{\rm b}$).

To perform all these measurements, one of us (YA) wrote the interactive code MIDE3700[5], in Python language. Its name corresponds to the Spanish acronym for Medición Interactiva de la Discontinuidad En 3700 Å (Interactive Discontinuity Measurement at 3700 Å). With this tool the user can work over the stellar spectrum and choose the best fits to Balmer and Paschen continua. The code then automatically delivers the values of D,

[1] The optical layout of this instrument is similar to the Boller & Chivens spectrograph offered for the du Pont 100-inch telescope of Las Campanas Observatory (Chile), http://www.lco.cl/telescopes-information/irenee-du-pont/instruments/website/boller-chivens-spectrograph-manuals/user-manual/the-boller-and-chivens-spectrograph

[2] http://www.eso.org/sci/observing/tools/calendar/ParAng.html

[3] IRAF is distributed by the National Optical Astronomy Observatory, which is operated by the Association of Universities for Research in Astronomy (AURA), Inc., under cooperative agreement with the National Science Foundation.

[4] http://www.casleo.gov.ar/info-obs.php

[5] The authors offer the code MIDE3700 to those whom wish to use it.

λ_1, and Φ_b and the corresponding fundamental parameters of a star.

From observed and intrinsic color gradients we estimated the color excess, $E(B-V) = 2.1\,(\Phi_b - \Phi_b^0)$ or $E(B-V) = 2.3\,(\Phi_{bb} - \Phi_{bb}^0)$, of each star and its distance modulus, using the apparent visual magnitude available in the literature. In addition, we calculated the stellar luminosity ($\mathcal{L}_\star/\mathcal{L}_\odot$), stellar mass ($M_\star/M_\odot$), and age of each star interpolating in the stellar evolutionary models, for a non-rotating case and $Z = 0.014$, provided by Ekström et al. (2012). For more details see Paper II.

From these data we derived for each open cluster, the true distance modulus, $(m_v - M_v)_0$, color excess $E(B-V)$, and age with their respective error bars. The distance modulus and memberships are calculated using an iterative procedure as explained in Paper II, based on the statistical distribution of individual distance modulus for the observed full sample of stars in the direction of each cluster. The first step is the calculation of a mean distance modulus (DM^0) and its standard deviation (σ^0). Then, we select a smaller sample that consist of stars with distance moduli at $1\sigma^0$ of DM^0. With this reduced sample we recalculate new values, which are the adopted mean true distance modulus of the cluster $DM_c = (m_v - M_v)_0$ and its standard deviation σ. The color excesses $E(B-V)$ are calculated using the same small sample.

The membership criterion is based on the distance modulus of each star and its error bars. When this distance modulus is outside the region defined by 3σ size around the mean cluster distance modulus, the star is considered a non-member (*nm*). If the star is inside a region between 2σ and 3σ size, the star is considered a probable non-member (*pnm*). If the star is between 1σ and 2σ size it is a probable member (*pm*) and if its distance modulus is less than 1σ size the star is considered as member (*m*).

On the other hand, cluster membership probabilities, p, of individual stars can be estimated using the statistical P-method approach. Assuming the null hypothesis is true, if the P-value is less than (or equal to) a given significance level, α, then the null hypothesis is rejected instead if the P-value is high it is accepted. As we are dealing with a rather modest number of objects in each cluster, to define a good distribution of distances we adopt the standard statistical level of significance of 5% to classify a star as a cluster member.

The cluster age was estimated from the HR diagram by setting the isochrones (Ekström et al. 2012) to the locations of the stars classified as members and probable members of the cluster. These stars are identified as *m* and *pm* in column 5 of Tables 10, 12, 14, and 16.

4. Results

For each cluster analyzed here, NGC 6087, NGC 6250, NGC 6383, and NGC 6530, we present a brief summary of previous studies and the results obtained with the BCD system of each individual star. This information is listed in two tables. The first table shows the star identification, observed BCD parameters D, λ_1, Φ_b, and stellar physical properties (spectral type and luminosity class, $T_{\rm eff}$, log g, M_v, $M_{\rm bol}$, and the intrinsic color gradient Φ_b^0). The BCD spectral types were tested, when it was possible with those of the standard MK system. On some occasions, we were not able to interpolate or extrapolate the BCD parameters because they were out of the range of the BCD calibrations. In those cases we used the MK-classification system to derive the spectral types and the corresponding fundamental parameters (Cox 2000). In addition, the intrinsic color gradients were estimated using the relation between Φ_b and $(B-V)$ given by Moujtahid et al. (1998).

The second table includes for each star: the visual apparent magnitude m_v, obtained color excess $E(B-V)$, true distance modulus $(m_v - M_v)_0$, angular distance to the cluster center AD, membership probability p, luminosity $\mathcal{L}_\star$ in solar units, stellar mass $M_\star$ (in unit of solar mass), and age. The coordinates of the cluster and their angular diameters were taken from Dias et al. (2002).

The cluster parameters are presented and discussed in the following subsections.

4.1. NGC 6087

NGC 6087 ($\alpha = 16^h18^m50$ and $\delta = -57°\,56\overset{m}{.}1$; J2 000) is located near the southern edge of the Normae constellation in a region that appears to be uniformly reddened near the Galactic plane (Sagar & Cannon 1997). It is one of the brightest open clusters in this region and it is very rich in Be stars. Several authors studied this cluster and its parameters were estimated with different techniques. In Table 3, the $E(B-V)$ values range from 0.13 mag to 0.22 mag and the cluster distance modulus is between 9.375 mag and 10.233 mag (750 pc $< d <$ 1000 pc). The cluster age presents big uncertainties, ranging from 10–20 Myr to 146 Myr.

The spectral classification of the stars in the region of NGC 6087 was performed only by Feast (1957) who reported the Hβ line in emission in star No. 10. Additional Be stars (Nos. 9, 14, and 22) were reported by Mermilliod (1982), while star No. 25 was classified as a CP2 star by Maitzen (1985) using the photometric Δa system.

Although some preliminary stellar parameters for this cluster were previously reported by Aidelman et al. (2010), we provide an improved set of BCD measurements (see Tables 9 and 10, available at the CDS) that were obtained with the MIDE3700 code and the new BCD M_v calibration given by Zorec & Briot (1991), instead of that reported by Zorec (1986). From these data we obtained the following cluster parameters: $(m_v - M_v)_0$ = 9.00 ± 0.19 mag, d = 629 ± 54 pc, and $E(B-V)$ = 0.35 ± 0.03 mag. As we derived a high value of $E(B-V)$ our distance modulus is slightly lower than those previously reported in the literature. We attribute this high $E(B-V)$ to particularities of the selected sample. Apart from the fact that many of the stars of the sample present evidence of circumstellar envelopes, the large $E(B-V)$ excess could be ascribed to the non-uniform dust distribution (see Fig. 1) revealed in the image from Wide-field Infrared Survey Explorer (WISE; Wright et al. 2010) $W3$ band (12 μm), where we identified our sample.

Considering our criterion for selecting star members (see Sect. 3), based on $(m_v - M_v)_0$ = 9.00 mag and σ = 0.5 mag, we find 12 star members (*m*, Nos. 1, 8, 9, 10, 11, 13, 14, 15, 25, 36, 128, and 156). Furthermore, taking into account the p values, we can confirm that stars Nos. 8, 9, 13, 14, 25, and 128 are cluster members (see Table 10), and stars Nos. 33 and 35 are non-members (*nm*).

On the other hand, according to the calculated angular distances and considering that the mean cluster diameter is 14′ (Dias et al. 2002), the most distant stars are Nos. 1 and 22.

In the literature we found that stars reported as *pnm* or *nm* are Nos. 7, 10, and 129 (Landolt 1964; Schmidt 1980; Turner 1986). However, as both Nos. 7 and 10 are Be stars (see Sect. 5), these authors could have been underestimated the absolute magnitudes due to the presence of the circumstellar envelope. From proper motion measurements Dias et al. (2014) classified stars Nos. 7,

Table 3. NGC 6087: previous and current determinations of color excess, distance, and age.

Reference	$E(B-V)$ [mag]	$(m_{\rm v}-M_{\rm v})_0$ [mag]	d [pc]	Age [Myr]
Trumpler (1930)^{sp}	...	...	870	...
Fernie (1961)^{ph}	0.22	9.4	750	10–20
Landolt (1963)^{ph}	0.20	9.8 ± 0.1	...	...
Breger (1966)^{ph}	0.20 ± 0.01	9.7	...	...
Graham (1967)^{ph}	...	9.9	950	...
Lindoff (1968)^{sc}	...	...	930	~41
Becker & Fenkart (1971)^{ph}	0.13	9.96	820	...
Tosi (1979)*	...	...	...	55 ± 5; 55 ± 9.6;146 ± 11
Schmidt (1980)^{ph}	$0.17 \pm 0.01^{**}$	9.60 ± 0.09	...	...
Janes & Adler (1982)^{ph}	0.21	10.23	...	~40
Turner (1986)^{ph}	...	9.78 ± 0.13	902 ± 10	...
Sagar (1987)^{ph,sp}	0.18 ± 0.05	9.8	...	20
Meynet et al. (1993)^{i}	...	...	...	~71
Sagar & Cannon (1997)^{ph}	0.22	...	1000 ± 100	65
Robichon et al. (1999)^{h}	...	...	769	...
Rastorguev et al. (1999)^{h}	...	...	820	...
Baumgardt et al. (2000)^{h}	...	...	819.67	...
Loktin & Beshenov (2001)^{h}	...	9.375	...	~95
Kharchenko et al. (2005)^{h}	...	...	901	~85
Piskunov et al. (2007)^{h}	0.18	...	...	...
An et al. (2007)^{ph}	0.132 ± 0.007	9.708 ± 0.048	...	...
This work	0.35 ± 0.03	9.00 ± 0.19	629 ± 54	~55

Notes. $^{(h)}$ Results based on Hipparcos data. $^{(i)}$ Results based on the isochrone fitting method. $^{(ph)}$ Results based on photometric data. $^{(sc)}$ Results based on synthetic clusters. $^{(sp)}$ Results based on spectroscopic data. $^{(*)}$ The age of the cluster was derived by three different methods: isochrone fitting, position of the turn-off point, and period of Cepheid stars (55 Myr, 146 Myr, and 55 Myr, respectively). The author argued that the most accurate method is the isochrone fitting followed by the Cepheid periods. $^{(**)}$ The color excess $E(B-V)$ was calculated in this work, using the $E(b-y)$ value given by Schmidt (1980) and the relation $E(b-y) = 0.74\,E(B-V)$.

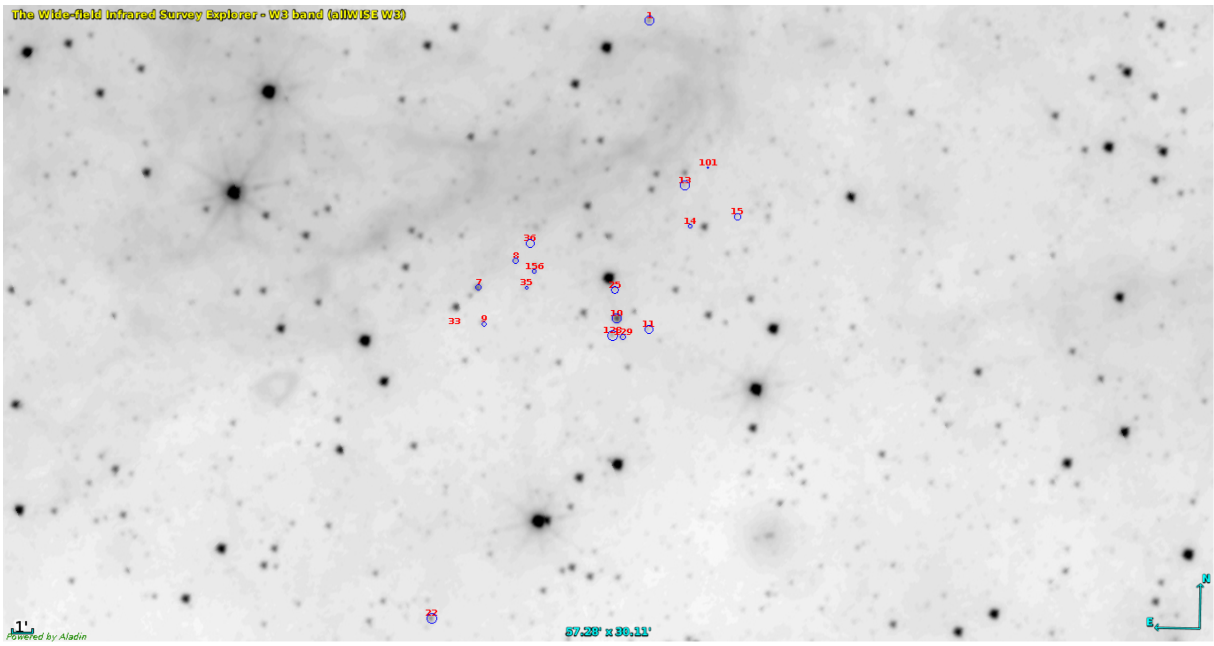

Fig. 1. NGC 6087: image from WISE W3 band showing a non-uniform dust distribution. The circles indicate the positions of the stars which are proportional to the measured $E(B-V)$.

8, 9, 10, 11, 13, 14, 15, 25, 128, 129, and 156, as members and assigned to star No. 35 a probability of 11%.

Our studied sample of stars defined well the cluster HR diagram over which we had plotted the isochrones for non-rotating star models given by Ekström et al. (2012, see Fig. 2). The Be star No. 22, classified as *pm*, is the most luminous object in the HR diagram and is located in the most external region of the cluster (see Fig. 1). This star was also classified as a blue

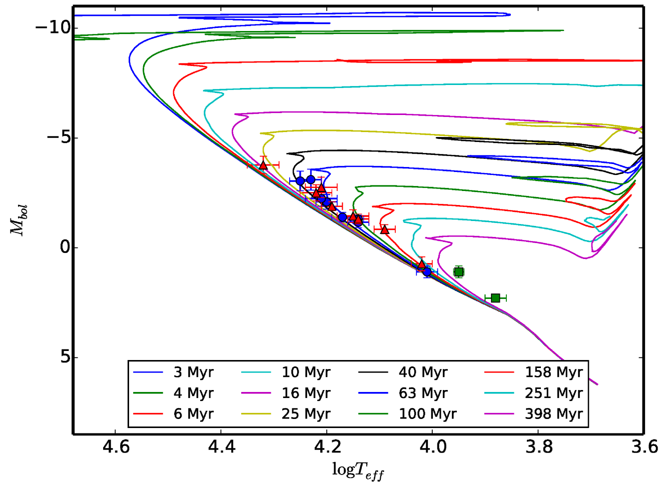

Fig. 2. NGC 6087: HR diagram. The estimated age for this cluster is ∼55 Myr. The isochrone curves are given by Ekström et al. (2012). Members and probable members of the clusters are denoted in blue circles and probable non-members and non-members in green squares. Star members with circumstellar envelopes are indicated in red triangles.

straggler. Therefore, if we do not consider this object in the sample, the inferred cluster age is ∼55 Myr. This value agrees very well with those obtained by Tosi (1979).

The BCD spectral types agree with the spectral classification reported by Feast (1957), considering the sample of stars that are in common. In addition, we determined the spectral type of four stars (Nos. 25, 33, 101, and 128) for the first time. In our sample we distinguish seven stars showing a SBD: Nos. 7, 9, 10, 11, 14, 101, and 156 (see Fig. 12).

4.2. NGC 6250

NGC 6250 (α = 16^{h}57^{m}58 and δ = −45°56$\overset{m}{.}$6; J2 000) has a peculiar distribution in the sky. The cluster consists of a very compact central region surrounded by sparse bright stars. Several arguments have suggested that the cluster is associated with a prominent dust cloud and is affected by differential reddening. Feinstein et al. (2008) identified several dust components along the light of sight and found that most of the stars do not show indications of intrinsic polarization.

Previous cluster parameters were estimated with various techniques (see Table 4) and they show a low scatter. The spectral classification of its individual members was performed by Herbst (1977) and a detailed chemical analysis of 19 upper main sequence stars was carried out by Martin et al. (2017). Star No. 35 is the only known Be star, star No. 34 was reported as peculiar (in He and in the K-line; Lodén & Nordström 1969), and star No. 3 as a visual binary (Herbst 1977).

The results obtained from MIDE3700 code are listed in Tables 11 and 12 (available at the CDS). From them we derived the mean cluster parameters $(m_{\rm v} - M_{\rm v})_0$ = 10.55 ± 0.33 mag, $E(B-V)$ = 0.38 ± 0.16 mag and d = 1 288 ± 210 pc. The obtained color excess is in very good concordance with those determined by Moffat & Vogt (1975) and Herbst (1977). Figure 3 is an image obtained in the W3 band that shows the dust distribution around the open cluster NGC 6250. The distance modulus agrees better with the determination performed by Piskunov et al. (2008).

From our membership criterion we found 8 members (Nos. 1, 2, 3, 17, 18, 35, 37, and HD 329 211) based on $(m_{\rm v} - M_{\rm v})_0$ = 10.55 mag and σ = 0.9 mag. Among these, stars Nos 1, 2 17, 35, 37, and HD 329 211 are confirmed members via their p values (see Table 12). Stars Nos. 21, 22, 33, 34, and CD−49 11096 are *pm*, star No. 32 is a probable non-member (*pnm*). Star No. 4, which has a low p value, is *nm* but it was reported as *pnm* by Moffat & Vogt (1975).

Our membership criterion agrees with the memberships derived from polarimetric measurements (Feinstein et al. 2008) and from proper motion determinations (Dias et al. 2014), in relation with those stars observed in common (Nos. 1, 2, 3, 17, and 18).

An inspection of the angular distances of the stars respect to the cluster center reveals that half of these stars are located out of the mean angular diameter assumed for the cluster (of 10′; Dias et al. 2002). Since stars Nos. 33, 34, and 35 are *m* or *pm* according to our membership criterion, one might think that the angular diameter of the cluster is larger than 10′. Extreme cases are CD−49 11096 and HD 329 211. We have not found any information regarding the memberships of these stars in the literature.

On the other hand, according to our HR diagram the cluster age is ∼6 Myr (see Fig. 4), which is lower than the values reported in the literature (see Table 4). To justify older ages with our data (by factors 2 or 4) we had to admit that we were overestimating effective temperatures by nearly 60%, corresponding to underestimations of the BD on the order of 0.1 dex, and this is impossible to admit. The age discrepancy we find is significant and could be due to the spectral type that different works considered as the earliest in their samples to determine the cluster age. In our work, we used stars of spectral type B0 to derive the age of the cluster, while Herbst (1977) and Battinelli & Capuzzo-Dolcetta (1991) used stars of spectral type B1 and Kharchenko et al. (2005) and McSwain & Gies (2005) instead took a sample of stars of spectral type B2. These spectral types imply $(T_{\rm eff}, \log L/L_{\odot})$ parameters that range from (4.48, 4.63) to (4.47, 4.89) for stars B0V to B0III, (4.43, 4.24) to (4.41, 4.53) for stars B1V to B1III and (4.35, 3.73) to (4.32, 4.1) for stars B2V to B2III. These $(T_{\rm eff}, \log L/L_{\odot})$ intervals identify isochrones in Fig. 4 near 6 Myr, 16 Myr, and 25 Myr, respectively, which correspond to the estimated ages by the different authors listed in Table 4.

The BCD spectral classification agrees with that performed by Herbst (1977) for 8 of the 12 stars we have in common. Furthermore, we derived for the first time a spectral classification for CD−49 11096. Only star No. 1 presents a SBD in its spectrum, which is in emission (see Fig. 12). This star has a high effective temperature ($T_{\rm eff} \simeq$ 27 400 K). From simple arguments based on the opacity of circumstellar envelopes of Be stars it is not possible to have conspicuous continuum emissions in the Balmer continuum near λ3600 Å without some emission in the first members of the Balmer series. The line emission in such classical Be stars is rarely very high. Unfortunately, the BCD spectrophotometric observations of this star did not extend up to the Hβ line. On the other hand, the spectroscopic observation carried out with REOSC shows H absorption line profiles (see Sect. 5.3), although low- and high-resolution observations are not simultaneous.

Finally, we confirm that No. 34 is peculiar and we classified it as a He-strong star. The star shows very intense lines of He I. We measured the following equivalent widths: EW_{4471} = 1.9 Å, EW_{4387} = 1.3 Å, EW_{4026} = 2.1 Å, which are about twice greater than those expected at the spectral type B0V (see Didelon 1982).

Table 4. NGC 6250: previous and current determinations of color excess, distance, and age.

Reference	$E(B-V)$ [mag]	$(m_v - M_v)_0$ [mag]	d [pc]	age [Myr]
Moffat & Vogt (1975)[ph]	0.38 ± 0.02	9.92*	950	···
Herbst (1977)[ph]	0.37	10.05	···	14
Battinelli & Capuzzo-Dolcetta (1991)[c]	···	···	···	~14
Kharchenko et al. (2005)[h]	···	···	865	~26
McSwain & Gies (2005)[ph]	0.35**	9.69	···	~26
Piskunov et al. (2008)[h]	0.35	10.77	···	···
This work	0.38 ± 0.16	10.55 ± 0.33	1 288 ± 210	~6

Notes. [(c)] Results based on catalogs. [(h)] Results based on Hipparcos data. [(ph)] Results based on photometric data. [(*)] The intrinsic distance modulus was calculated in this work, using $(m_v - M_v)$ and $E(B-V)$ values published by Moffat & Vogt (1975) with $R_v = 3.1$. [(**)] The color excess $E(B-V)$ was calculated in this work, using the $E(b-y)$ value given by McSwain & Gies (2005) and the relation $E(b-y) = 0.74\,E(B-V)$.

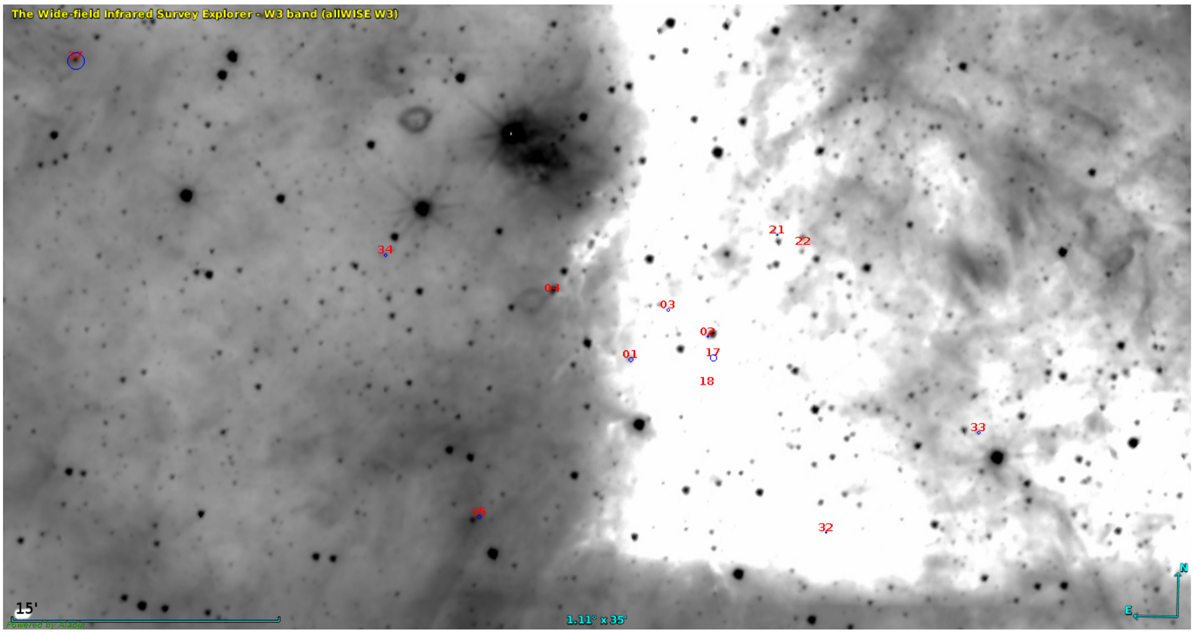

Fig. 3. Idem Fig. 1 but for NGC 6250. Stars HD 329 211 and CD−49 11096 are not included because of its large angular distance from the center of the cluster.

4.3. NGC 6383

NGC 6383 ($\alpha = 17^h34^m48$ and $\delta = -32°\,34\overset{m}{.}0$; J2 000) is a rather compact open cluster, which could be part of the Sgr OB1 association together with NGC 6530 and NGC 6531 (cf. Rauw & De Becker 2008). The brightest star HD 159 176 is a well-studied X-ray double-line spectroscopic binary responsible for the ionization of the H II region RCW 132.

This cluster was widely studied with different techniques (see Table 5). In contrast to other studied clusters, the spectral classification of the star members was performed by several authors (The 1966; Antalová 1972; Lloyd Evans 1978; The et al. 1985; van den Ancker et al. 2000). This cluster has many Be and peculiar stars: Nos. 1 and 100 were reported as double-line spectroscopic binaries (Trumpler 1930; Sahade & Berón Dàvila 1963, respectively) while Nos. 14 and 83 were reported as possible spectroscopic binaries (Lloyd Evans 1978). No. 3 was reported as an Ap spectroscopic variable (The et al. 1985; Landstreet et al. 2008). Stars Nos. 1 and 6 were classified as blue stragglers and, in particular, No. 1 was also classified as emission-line star. Star No. 76 was reported to have Hα in emission.

Tables 13 and 14 (available at the CDS) list the derived stellar parameters and from these we infer the following cluster parameters: $(m_v - M_v)_0 = 9.61 \pm 0.38$ mag, $E(B-V) = 0.51 \pm 0.03$ mag, and $d = 834 \pm 158$ pc. The derived color excess is higher than previous published values, therefore our distance estimate is lower. We attribute this high value to the special characteristics of the selected sample; i.e., most of the stars have circumstellar envelopes and are located in a dense dusty region (see Fig. 5).

Considering the values $(m_v - M_v)_0 = 9.61$ mag and $\sigma = 1.13$ mag we classified 8 star members (Nos. 1, 2, 10, 14, 57, 76, 83, and 100), 2 as *pm* (Nos. 3 and 6) and 2 as *pnm* (Nos. 47 and 85, both are the coolest stars of this sample). Stars Nos. 1, 2, 14, 76, and 83 are also members according to our p-method criterion. Star No. 85 was reported as *nm* by Lloyd Evans (1978). The stars classified as *m* and *pm* also present *AD* lower than the cluster angular diameter (of 20′; Dias et al. 2002). Moreover, based on proper motion measurements, stars Nos. 1, 2, 3, 6, 10, 14, 47, 57, 83, and 100 were considered members by Dias et al. (2014) while star No. 85 has a 1% of probability. Then we have 1 star in discrepancy with Dias et al. (2014, No. 47).

The cluster HR diagram is very well defined and the derived cluster age, ~3 Myr, agrees with the most of

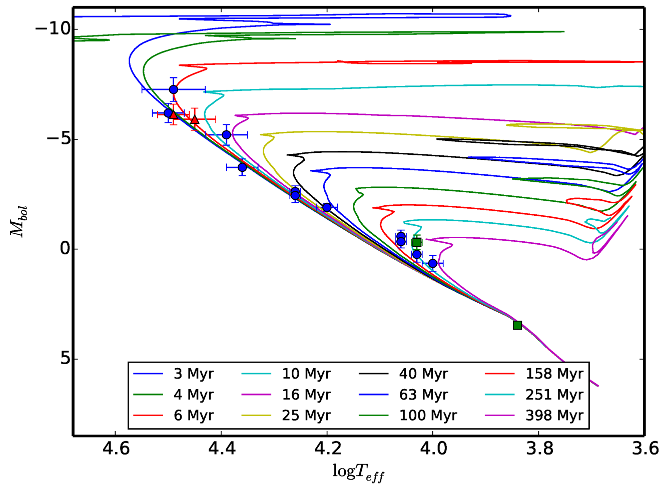

Fig. 4. NGC 6250: HR diagram. The estimated age for this cluster is ∼6 Myr. The isochrone curves are given by Ekström et al. (2012). Members and probable members of the clusters are denoted in blue circles and probable non-members and non-members in green squares. Star members with circumstellar envelopes are indicated in red triangles.

the values found in the literature (Fitzgerald et al. 1978; Battinelli & Capuzzo-Dolcetta 1991; Kharchenko et al. 2005; Paunzen et al. 2007). However, if we consider that star No. 6 has started to evolve (see Fig. 6, second more bright star of the sample) and accept that the X-Ray Be binary star No. 1 (HD 159 176) is a blue straggler, then the age of the cluster is between 6 Myr and 10 Myr.

Our spectral classification agrees with those found in previous works, in particular with Lloyd Evans (1978). We observed a SBD in absorption in the spectrum of star No. 57 (see Fig. 12).

4.4. NGC 6530

NGC 6530 (α = 18^{h}04^{m}31 and δ = −24°21$'$.5; J2 000) is a very young cluster located in the H II region M8, also known as the Lagoon Nebulae, near the Sagittarius-Carina spiral Galactic arm. Several authors studied this cluster and its parameters were estimated with different techniques (see Table 6). The color excess $E(B-V)$ and the cluster distance have large uncertainties, with values between 0.30 mag and 0.541 mag and between 730 pc and 1900 pc, respectively. However, the cluster age is better defined because it is less than 7 Myr.

The spectral classification of the individual star members was performed by Walker (1957); Hiltner et al. (1965); Chini & Neckel (1981); Torres (1987); Boggs & Bohm-Vitense (1989), and Kumar et al. (2004). The cluster has many variable stars and many emission-line stars. Stars Nos. 7, 9, 56, 65, 86, and 100 were reported as spectroscopic binaries, and Nos. 43 and 73 as triple systems. In addition, stars Nos. 42, 45, 56, 60, 65, and 100 show H lines in emission, however, it is still under debate whether these emissions originate in the H II region or in a circumstellar envelope. On the other hand, Kumar et al. (2004) reported star No. 65 as a Herbig Ae/Be I or III, and Niedzielski & Muciek (1988) classified star No. 59 as an unknown peculiar type and star No. 66 as a He-weak. Finally, stars Nos. 73 and 93 were reported as blue stragglers.

With the BCD system we derived the stellar fundamental parameters (Tables 15 and 16, available at the CDS) and the mean cluster parameters: $(m_v - M_v)_0$ = 11.76 ± 0.20 mag, $E(B-V)$ = 0.26 ± 0.05 mag, and d = 2245 ± 215 pc. The distance modulus agrees very well with the determination carried out by Lindoff (1968), but our derived color excess is systematically lower than previous published values. Figure 7 displays a W3-band image in the surroundings of NGC 6530 together with our color excess determinations. The low $E(B-V)$ values we derived indicate that the dusty region is located behind the cluster.

Taking into account our membership criterion (with $(m_v - M_v)_0$ = 11.76 mag and σ = 0.78 mag) we found 15 members (Nos. 32, 42, 43, 56, 60, 61, 65, 66, 68, 70, 73, 76, 86, 93, and 100), 6 *pm* (Nos. 7, 9, 45, 55, 59, and 85), and 2 *nm* (No. 80 and LSS 4627). We can confirm as cluster members stars Nos. 43, 65, 70, and 86 because they have high p values. On the other hand, LSS 4627 is the star farthest from the center of the cluster and we considered it as a *nm*. The rest of stars have angular distances lower than the cluster angular diameter of 14$'$ (Dias et al. 2002). We have 17 stars in common with Dias et al. (2014, Nos. 32, 42, 43, 55, 56, 59, 60, 61, 65, 66, 68, 70, 73, 76, 80, 86, and 93) who considered all of these stars as members. Therefore, only star No. 80 is in discrepancy.

Even though, the stars show some scatters in the HR diagram (probably due to the binary nature of many stars in the cluster), the cluster age seems to be about 4–6 Myr (see Fig. 8). This value agrees with most of the previous determination.

Our spectral classification confirms that performed by Hiltner et al. (1965); Chini & Neckel (1981); Torres (1987), and Boggs & Bohm-Vitense (1989). Stars No. 68 (B0V) and LSS 4627 (B1V) have been classified for the first time. The former exhibits a narrow emission in the Hβ core that could be attained to a nebular contribution. We find that star No. 9 has an anomalous color excess for its spectral type. We observed a SBD in the spectra of stars Nos. 45 and 65. This confirms that star No. 65 is a Be star, which is shown in Fig. 12. Instead, we found that star No. 45 is a supergiant. According to the location of stars Nos. 73 and 93 in the HR diagram, they cannot be classified as blue stragglers.

5. Population of B, Be, and Bdd stars

We used the BCD method to derive physical properties of a large number of stars (∼230) in the direction of the open clusters Collinder 223, Hogg 16, NGC 2645, NGC 3114, NGC 3766, NGC 4755, NGC 6025, NGC 6087, NGC 6250, NGC 6383, and NGC 6530 (see Paper I, Paper II and this work). Thus, we gathered a homogeneous set of fundamental parameters that in addition are not affected by the interstellar or circumstellar reddening. This way we were able to obtain cluster parameters of 11 open clusters, construct well-defined HR diagrams and perform a better identification of the cluster star members. At the same time, the study of the BD enables the detection of circumstellar envelopes around B-type stars in an independent way from the typical criterion based on the presence of emission H lines. This is possible through the observation of a SBD.

In this section, we discuss the derived BCD stellar fundamental parameters and describe the main characteristics of the population of B stars. Particularly, we present global properties of stars with circumstellar envelopes.

5.1. The BCD stellar fundamental parameters

The discussion of the fundamental parameters is based on a reduced sample of 198 early-type stars, classified as members (m) and probable members (pm) of the 11 open clusters studied. We discarded pnm or nm stars from this analysis.

Table 5. NGC 6383: previous and current determinations of color excess, distance, and age.

Reference	$E(B-V)$ [mag]	$(m_v - M_v)_0$ [mag]	d [pc]	Age [Myr]
Trumpler (1930)^{sp}	···	···	2130	···
Zug (1937)^{ph}	···	···	2130	···
Sanford (1949)^{sp}	···	···	760	···
Eggen (1961)^{ph}	···	···	1259	···
Graham (1967)^{ph}	···	10.68 ± 0.54	1380	···
Lindoff (1968)^{ph}	···	10.5	1250	∼20
Becker & Fenkart (1971)^{c}	0.26	10.92	1065	···
Fitzgerald et al. (1978)^{ph,sp}	0.33 ± 0.02	10.85	1500 ± 200	1.6 ± 0.4
Lloyd Evans (1978)^{ph}	0.35	10.6	1350	···
The et al. (1985)^{ph}	0.30 ± 0.01	···	1400 ± 150	···
Pandey et al. (1989)^{ph}	0.35	11.65	···	∼4
Battinelli & Capuzzo-Dolcetta (1991)^{sp}	···	···	1380	∼4
Feinstein (1994)^{ph}	0.33	···	1400	···
Rastorguev et al. (1999)^{h}	···	···	1180	···
Kharchenko et al. (2005)^{h}	···	···	985	∼5
Paunzen et al. (2007)^{ph}	0.28**	···	1700	4
Piskunov et al. (2008)^{h}	0.30	10.897	···	···
Rauw & De Becker (2008)^{ph}	0.32 ± 0.02	···	1300 ± 100	···
This work	0.51 ± 0.03	9.61 ± 0.38	834 ± 158	∼3–10

Notes. $^{(c)}$ Results based on catalog data. $^{(h)}$ Results based on Hipparcos data. $^{(ph)}$ Results based on photometric data. $^{(sp)}$ Results based on spectroscopic data. $^{(**)}$ The color excess $E(B-V)$ was calculated in this work, using the published $E(b-y)$ value and the relation $E(b-y) = 0.74\,E(B-V)$.

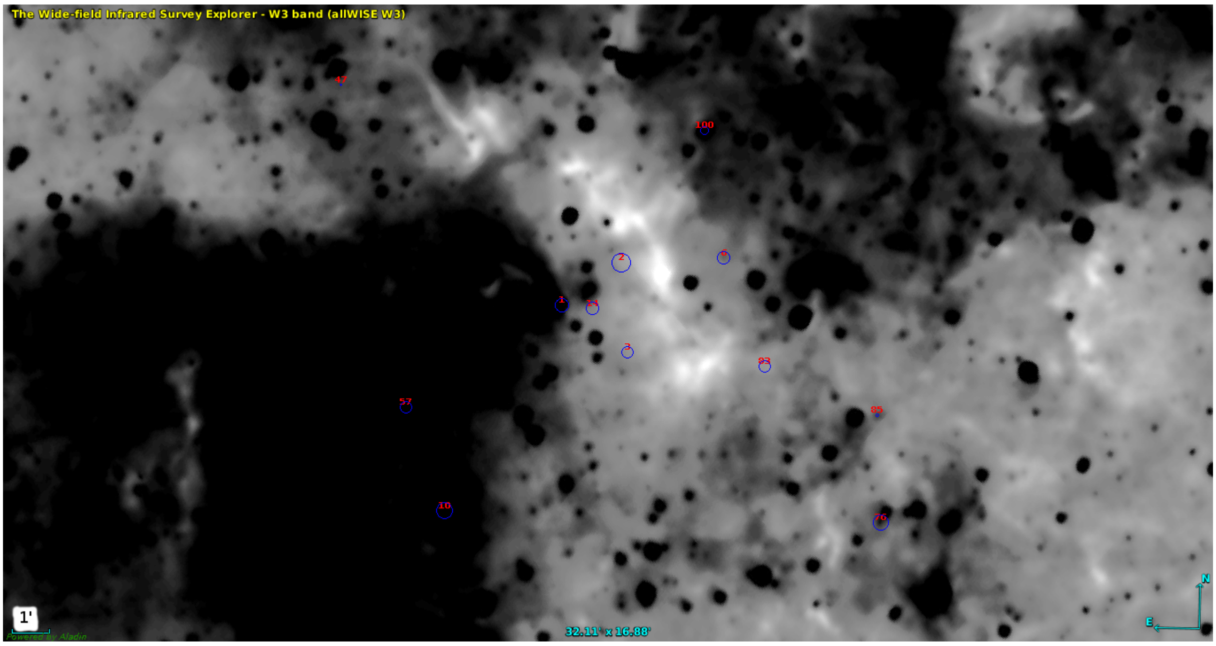

Fig. 5. Idem Fig. 1 but for NGC 6383.

Firstly, we compared the BCD fundamental parameters of all the stars, T_{eff} and M_v, with the scarce values reported in the literature. This comparison is shown in Fig. 9 where we distinguish normal B-type stars (identified with circles) from those that have circumstellar envelopes (identified with triangles). The effective temperatures were taken from McSwain et al. (2008, 2009, NGC 3766), Dufton et al. (2006, NGC 4755), Piskunov (1980, NGC 6025), and van den Ancker et al. (2000, NGC 6383). Whilst the absolute visual magnitudes were gathered from Clariá & Lapasset (1991, Collinder 223), Fitzgerald et al. (1979b, Hogg 16), Fitzgerald et al. (1979a, NGC 2645), Shobbrook (1985, NGC 3766), Kilambi (1975, NGC 6025), and Lloyd Evans (1978, NGC 6383)[6].

In relation to the BCD T_{eff} values (see Fig. 9a), in general they are systematically greater than those derived by other

[6] We only consider works that explicitly published M_v values for individual stars.

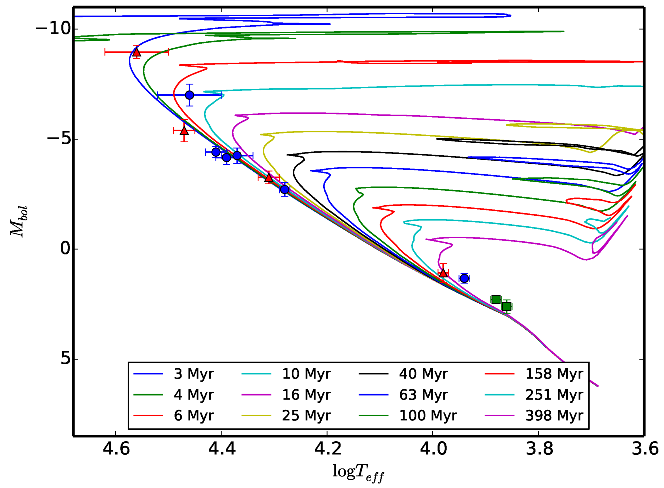

Fig. 6. NGC 6383: HR diagram. The estimated age for this cluster is between 3 and 10 Myr. The isochrone curves are given by Ekström et al. (2012). Members and probable members of the clusters are denoted in blue circles and probable non-members and non-members in green squares. Star members with circumstellar envelopes are indicated in red triangles.

techniques. It has been shown that the effective temperatures derived with the BCD method have no significant differences with the values derived from multicolor photometric systems, line-blanketed models, and infrared flux method (Cidale et al. 2007). Therefore, we observe that our $T_{\rm eff}$ determinations show discrepancies of about $\Delta T_{\rm eff} \lesssim 2000$ K, with those obtained by McSwain et al. (2008, 2009, Hα and Strömgren photometry) and Dufton et al. (2006, non-LTE atmospheric models). Instead, significant discrepancies are observed in some of the stars of NGC 6025. On the other hand, we have three stars in common with van den Ancker et al. (2000) and only the star NGC 6383 6 shows a huge discrepancy. Perhaps, this could be due to the too late spectral classification assigned to this star by these authors.

Regarding the $M_{\rm v}$ values, we have to consider that in most of the cases these were calculated using the distance modulus of the cluster. Therefore, we can only compare values obtained for stars belonging to clusters that have similar $(m_{\rm v} - M_{\rm v})_0$ as ours. Such clusters are Collinder 223, NGC 3766, NGC 6025, and NGC 6383. This comparison is shown in Fig. 9b. The greatest discrepancies, which means values with $|M_{\rm v_{BCD}} - M_{\rm v_{lit}}| > 2$ mag, are found among stars reported as Em, Be, supergiant, or variable[7]. It worth mentioning that most of the cited works consider average values of $E(B-V)$ and these could lead to the discrepancies observed in stars with circumstellar envelopes.

In relation to comparisons of absolute bolometric magnitudes and surface gravities (see Fig. 10) derived from stellar evolution models with the BCD parameters, we recognize that both show the same trends as found in Paper I. In that case, only the results for NGC 3766 and NGC 4755 were considered. We highlight the excellent agreement between BCD and evolutive $M_{\rm bol}$ values as is depicted in Fig. 10a. Whilst the discrepant behavior in log g (see Fig. 10b) was already mentioned in Paper I and it is related to the technique used to derive the surface gravity. The log g values derived from the BCD method (log $g(\lambda_1, D)$) are also called atmospheric gravities, since the BCD calibration of this quantity is based on parameters log g determined by fitting observed Hγ and Hβ lines with synthetic line profiles, obtained with classical model atmospheres. On the contrary, log $g_{\rm evol}$ are calculated using bolometric magnitudes $M_{\rm bol}(\lambda_1, D)$ and effective $T_{\rm eff}(\lambda_1, D)$ obtained from the BCD calibrations, which produce estimates of the stellar radius $R/R_\odot$, while they lead to masses $M/M_\odot$ obtain from the stellar evolutionary tracks. For stars with $M \lesssim 12\,M_\odot$ and radii $R \lesssim 12\,R_\odot$, the value of log $g_{\rm evol}$ is often estimated in the deep stellar layers while log $g_{\rm atm}$ is more related to the outermost atmospheric layers. A reverse situation would occur for evolved massive stars with $M \gtrsim 20\,M_\odot$ and $R \gtrsim 40\,R_\odot$.

The observed deviation between the log $g_{\rm evol}$ and log $g(\lambda_1, D)$, mostly at log $g \lesssim 3.7$ has already been noted by Gerbaldi & Zorec (1993) for late B- and early A-type stars. This deviation is due to an overestimate of the stellar mass possibly carried by difficulties with the stellar structure calculations at the helium ionization region (Maeder, priv. comm.).

It is worth noting that rotation, whose effects are neglected in the present analysis, would act with systematic differences in the log g determinations that range in the opposite way as noted above for stars with $M \lesssim 12\,M_\odot$. The log g corrected for rapid rotation effect, called pnrc (parent non-rotating counterpart) surface gravities (Frémat et al. 2005), are generally larger by about 0.14 ± 0.14 dex than the observed or apparent surface gravities. However, differences are largely aspect-angle dependent (Zorec et al. 2016).

Therefore, we should find higher apparent bolometric luminosities and lower effective temperatures than those expected for non-rotating stellar counterparts (Frémat et al. 2005; Zorec et al. 2005). As a consequence, we have lower log $g_{\rm evol}$ determinations than the values for non-rotating cases.

5.2. Balmer discontinuity of Be stars

The photospheric component of the BD is determined by the flux ratio $D_* = \log(F^+_{3700}/F^-_{3700})$. The value F^+_{3700} is given by the interception of the extrapolated straight line "A" that fits the Paschen continuum, shown in Fig. 11, and a vertical line at $\lambda = 3\,700$ Å and F^-_{3700} is given by the interception of same vertical line and the envelope curve "B" that passes over the absorption cores of the higher members of the Balmer lines until the point at which they merged.

Let us recall some characteristics of these fluxes:

1) The value F^+_{3700} represents the flux density that would exist if the wings of the higher members of the Balmer lines series (H$_n$; $n > 8$) did not overlap. This line overlapping produces a pseudo-continuum; this is represented by the last Balmer lines merged at redward with the upper curve "C" surrounding the Balmer lines in Fig. 11. Because of this overlap and the low resolution of the spectra, the last Balmer lines merged redward to the theoretical value, $\lambda \sim 3\,648$ Å.
2) This pseudo-continuum also intercepts the Balmer continuum shortly after the BD in O-, B-, A-, F-type stars without circumstellar emission or absorption.
3) The value F^-_{3700} also belongs to the above-mentioned pseudo-continuum, and as both fluxes $F^\pm_{3700}$ are measured at the same wavelength they are affected by nearly the same amount of emission or absorption, ΔF_{3700}, originated by a circumstellar envelope. For this reason, Papers I and II of this series

[7] These stars are Cr 223 35 (reported as blue straggler), Hogg 16 2 (reported as Em), Hogg 16 3 (reported as Em), Hogg 16 9 (reported as Em), NGC 2645 1 (classified as supergiant), NGC 2645 2 (classified as supergiant), NGC 3766 15 (reported as Be), NGC 3766 232 (reported as variable), NGC 3766 291 (reported as Be), NGC 6383 6 (reported with an IR excess), and NGC 6383 47 (classified as a bright giant).

Table 6. NGC 6530: previous and current determinations of color excess, distance, and age.

Reference	$E(B-V)$ [mag]	$(m_v - M_v)_0$ [mag]	d [pc]	Age [Myr]
Trumpler (1930)[ph]	···	···	1 090	···
Sanford (1949)[sp]	···	···	730	···
Johnson et al. (1961)[ph]	0.32	10.7 ± 0.3	1 400	···
Penston (1964)[p]	···	···	···	~1
Lindoff (1968)[sc]	···	11.91	1 560	<7
van Altena (1972)[ph]	0.35	11.25	1 780	2
Harris (1976)[sp]	···	···	···	6.36 ± 0.34
Kilambi (1977)[ph]	0.34	10.7	···	···
Sagar & Joshi (1978)[ph]	0.35	11.3	···	2
Chini & Neckel (1981)[ph,sp]	0.36 ± 0.09	11.4	···	···
Boehm-Vitense et al. (1984)[sp]	···	···	···	5 ± 2
Sagar et al. (1986)[ph]	···	···	···	~2
Battinelli & Capuzzo-Dolcetta (1991)[p]	0.35	···	1 600	~2
Strobel et al. (1992)[p]	0.4	12.7	···	~3
Feinstein (1994)[ph]	0.36	11.4	1 900	···
van den Ancker et al. (1997)[ph,sp]	0.30	···	1 800 ± 200	···
Rastorguev et al. (1999)[h]	···	···	1 270	···
Robichon et al. (1999)[h]	···	···	~763.36	···
Sung et al. (2000)[ph]	0.35	11.25 ± 0.1	···	1.5
Baumgardt et al. (2000)[h]	···	···	~917.43	···
Loktin & Beshenov (2001)[h]	···	9.005 ± 0.255	···	~7.5
Prisinzano et al. (2005)[ph]	···	···	1 250	2.3
Kharchenko et al. (2005)[h]	···	···	1 322	~4.7
McSwain & Gies (2005)[ph]	0.34**	10.62	···	~7.4
Zhao et al. (2006)[ph]	···	···	1 330	~7.4
Mayne & Naylor (2008)[p]	0.32	10.34	···	2
Kharchenko et al. (2009)[h]	0.30	···	1 322	~4.7
Kharchenko et al. (2013)[h]	0.541	···	1 365	~4.7
This work	0.26 ± 0.05	11.76 ± 0.20	2 245 ± 215	4–6

Notes. [(h)] Results based on Hipparcos data. [(p)] Results based on published data. [(ph)] Results based on photometric data. [(sc)] Results based on synthetic clusters. [(sp)] Results based on spectroscopic data. [(**)] The color excess $E(B-V)$ was calculated in this work, using the published $E(b-y)$ value and the relation $E(b-y) = 0.74\,E(B-V)$.

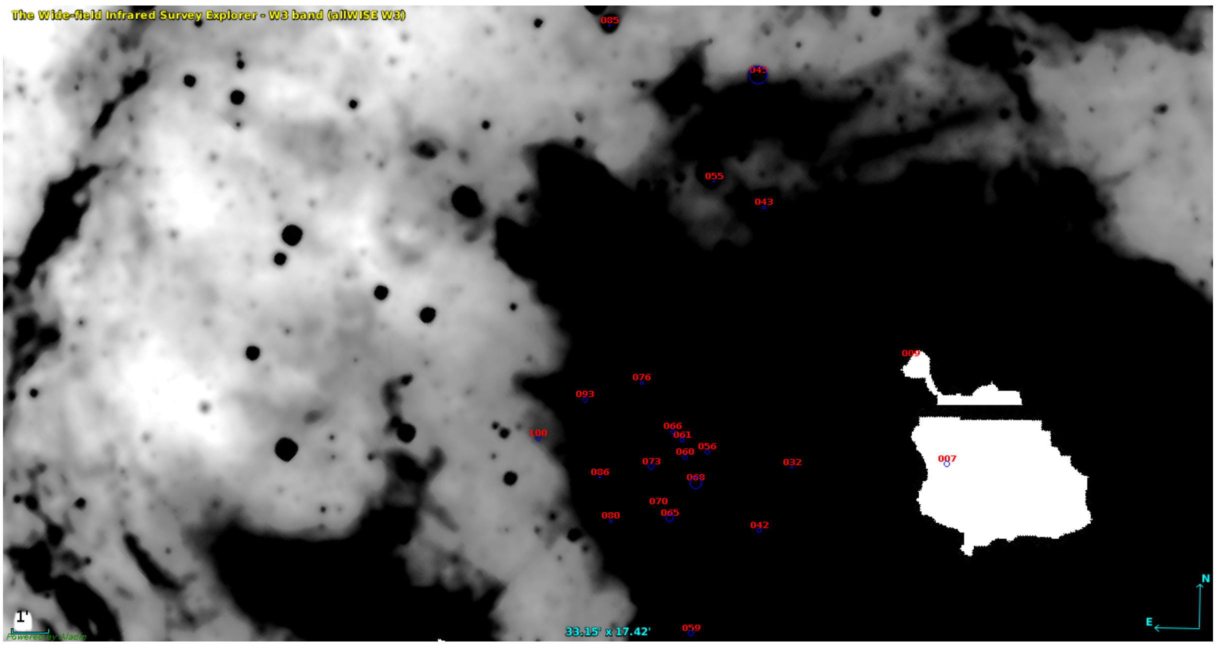

Fig. 7. Idem Fig. 1 but for NGC 6530. The image is saturated (white patch).

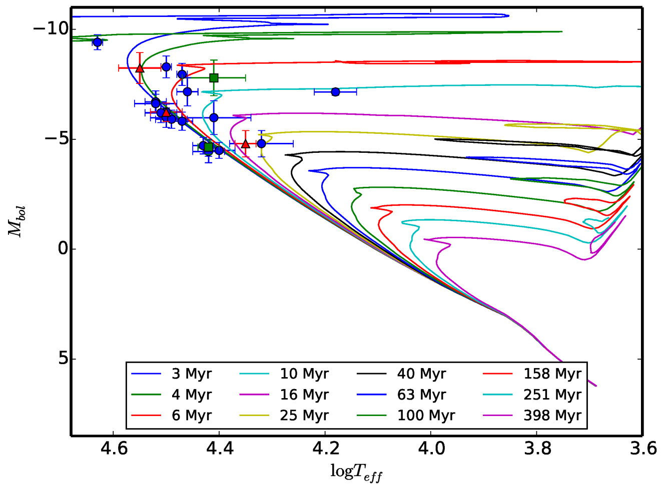

Fig. 8. NGC 6530: HR diagram. The estimated age for this cluster is 4–6 Myr. The isochrone curves are given by Ekström et al. (2012). Members and probable members of the clusters are denoted in blue circles and probable non-members and non-members in green squares. Star members with circumstellar envelopes are indicated in red triangles.

explain our care in determining where the last lines of the Balmer series overlap. The circumstellar emission or absorption have very little if any incidence on the determination of the photospheric BD, D_*. Therefore, the BD of some stars with circumstellar envelopes can be defined as the quantity $D = D_* + d$, where D_* is the height of the photospheric (or first) component of the BD and d represents the height of the SBD. The first component of the BD (D_*) has always been observed constant in Be stars, within the limits of uncertainties of the BCD system (0.015 dex in D and 1–2 Å in λ_1; De Loore et al. 1979; Divan et al. 1983; Divan & Zorec 1982; Zorec 1986; Zorec et al. 1989; Zorec & Briot 1991; Vinicius et al. 2006; Cochetti et al. 2013, 2015). Apart from the rare case of γ Cas (O9Ve, HD 5394) in 1935 and 1938 (Barbier & Chalonge 1939), the constancy of D_* has even been noted in stars with Be $\rightleftarrows$ B $\rightleftarrows$ Be-shell-phase changes such as γ Cas, Pleione, 88 Her, and 59 Cyg.

However, as D_* is determined empirically, it does not avoid two very small effects caused by the presence of a circumstellar envelope, i.e.,

a) The genuine photospheric fluxes $F^{\pm}_{3700}$ transform into $F^{\pm}_{3700}$ $+\Delta F_{3700}$, such that

$$D^{\rm obs}_* \simeq D^{\circ}_* + \left(\frac{\Delta F_{3700}}{F^{+}_{3700}}\right)\left(1 - 10^{D^{\circ}_*}\right), \qquad (1)$$

where D°_* represents the actual photospheric BD, which in the hottest stars is

$$\Delta F_{3700}/F^{+}_{3700} \lesssim 0.05. \qquad (2)$$

b) On the other hand, since F^{+}_{3700} is obtained by extrapolation, it is affected by the color effects in the Paschen continuum carried by the λ^3 dependency of the circumstellar envelope opacity. Moujtahid et al. (1998, 1999) and Gkouvelis et al. (2016) estimated these effects and obtained that

$$D_* = D^{\rm obs}_* + \epsilon_D$$

with $\qquad (3)$

$$\epsilon_D \simeq 0.02 \times [\Phi^{\rm obs} - \Phi(\lambda_1, D^{o}_*)],$$

As the compilation made by Moujtahid et al. (1998) actually corresponds to spotted measurements concerning otherwise long-term Be star "bumper" activity (Cook et al. 1995; Hubert & Floquet 1998; Hubert et al. 2000; Keller et al. 2002; Mennickent et al. 2002; de Wit et al. 2006) the color changes are on the order of $\Phi^{\rm obs} - \Phi(\lambda_1, D^{\circ}_*) \lesssim 0.5\,\mu$m and the error committed by this effect on the estimate of the photospheric BD is $\epsilon_D \lesssim$ 0.010 dex. This error carries uncertainties on the estimate of the visual absolute magnitude, which is smaller than the deviations of the absolute magnitude within a spectral type-luminosity class curvilinear box of the BCD system (Chalonge & Divan 1973; Zorec et al. 2009).

The SBD is caused by the flux excess produced in the circumstellar envelope due to bound-free and free-free transitions, mostly of hydrogen and helium atoms and electron scattering. On the other hand, spectrophotometric variations of Be stars are currently different according to the Be phases. Thus, emission phases ($d < 0$) are generally accompanied by a brightening and reddening of the Paschen continuum, while shell phases ($d > 0$) generally show little decreases of stellar brightening without changing the color of the Paschen continuum. An extensive compilation of these spectrophotometric behaviors was published by Moujtahid et al. (1998).

The height of the SBD, d, is then measured as the flux difference (in a logarithmic scale) between the observed Balmer continuum fitted by a straight-line "E" and a parallel line "F" to Balmer continuum through the point defined by the merged of the Balmer lines provides a measurement of d (see Fig. 11).

5.3. Stars with circumstellar envelopes

During the process of seeking emission-line stars in the direction of the 11 studied open clusters we found a total of 46 Be stars when considering the whole sample of 230 stars; this included 6 new Be stars, i.e., Cr 223 2, NGC 2645 5, NGC 3766 301, HD 308 852, NGC 6087 7, and NGC 6383 76[8]. Among these 46 Be stars, we detected 19 objects with a SBD.

In addition, we found 15 B-type stars with a SBD that show neither line emission features nor have been previously reported as Be stars and 3 B supergiants (BSG) with a SBD (HD 74 180, NGC 4755 1, NGC 6530 45). The 15 B-type stars that show a SBD could be Be candidates; we classified these stars as Bdd. In this way, the total number of stars with a SBD (Bdd+Be+BSG stars) is 37, which were identified in the corresponding tables of Papers I, II, and this work with a supra index dd; stars NGC 3766 55 and NGC 3114 126 were discarded since they have a doubtful SBD. Therefore, our whole sample of objects with a SBD in absorption consists of 29 stars (3 in Cr 223, 1 in Hogg16a, 2 in NGC 2645, 10 in NGC 3114, 1 in NGC 3776, 1 in NGC 4755, 2 in NGC 6025, 7 in NGC 6087, 1 in NGC 6383, and 1 in NGC 6530) and 8 in emission (2 in Cr 223, 1 in Hogg16b, 2 in NGC 3776, 1 in NGC 4755, 1 in NGC 6250, and 1 in NGC 6530).

Henceforth we restrict ourselves to studying the sample of Be and Bdd stars belonging to the 11 studied galactic clusters.

[8] We observe Hα in emission in the spectrum of these stars.

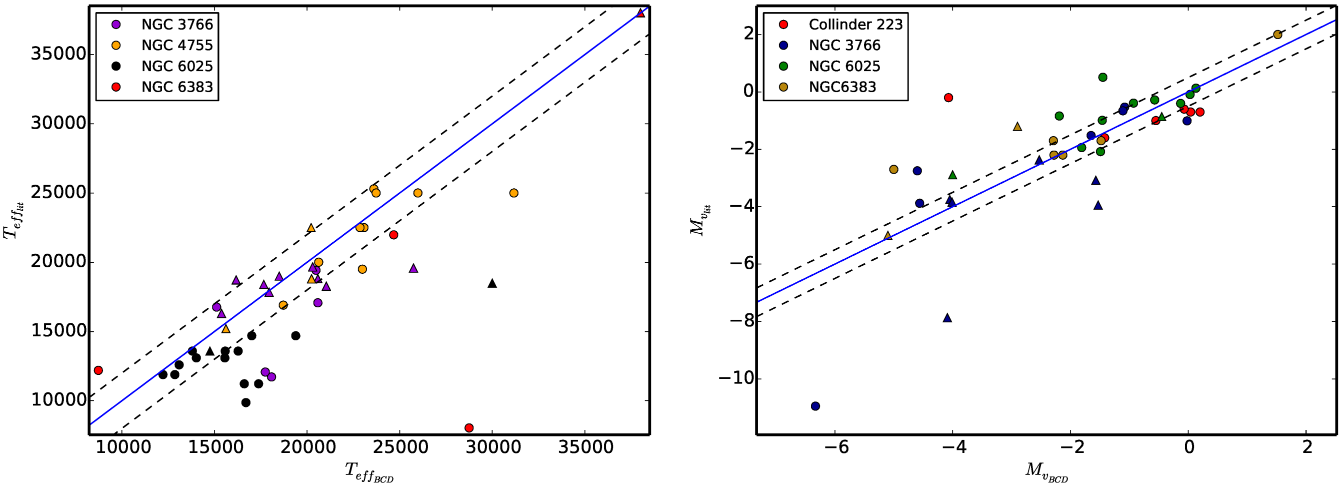

(a) Comparison of effective temperatures.

(b) Comparison of absolute visual magnitudes.

Fig. 9. Comparison of BCD $T_{\rm eff}$ and $M_{\rm v}$ values determined for member stars with those determined in previous works. The straight line is the identity function and the dotted lines deviate from it in 2000 K and 0.5 mag, respectively. The circles identify normal B-type stars and triangles are used for stars with circumstellar envelopes.

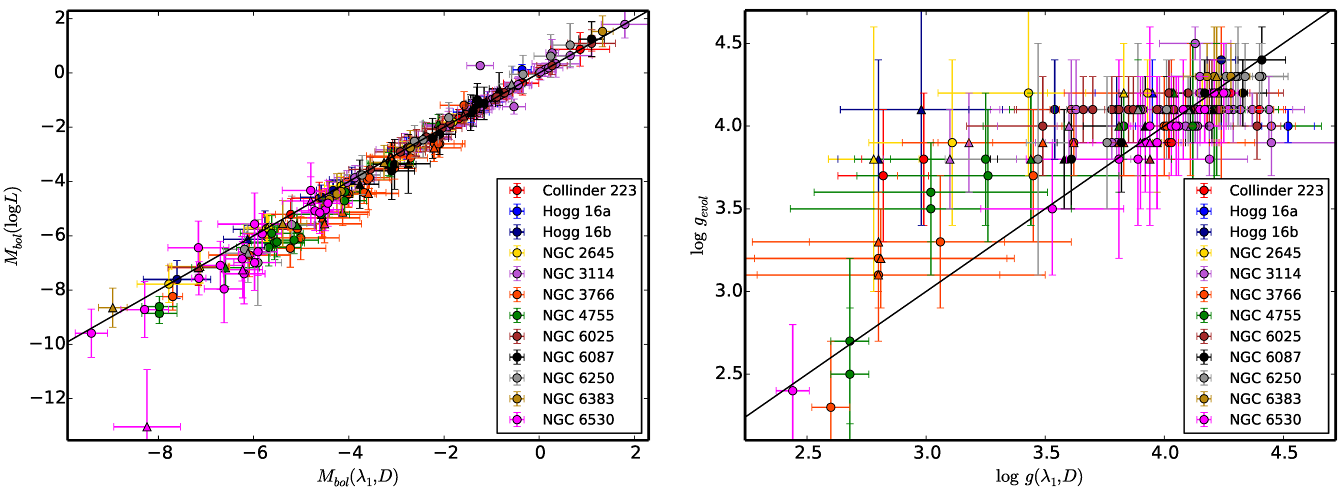

(a) Comparison of absolute bolometric magnitudes.

(b) Comparison of surface gravities.

Fig. 10. Comparison of $M_{\rm bol_{evol}}$ and $\log g_{\rm evol}$ parameters, derived from stellar evolution models, against BCD $M_{\rm bol}(\lambda_1, D)$ and $\log g(\lambda_1, D)$ estimates. Circles identify normal B-type stars and triangles stars with circumstellar envelopes. The straight line corresponds to the identity function.

This sample includes 42 Be (17 with a SBD) and 13 Bdd stars, mainly of B-type stars, although a few late O and early A stars were also observed. Among the 42 Be stars we found 30 dwarfs (e.g., luminosity classes IV, V, and VI) and 12 slightly more evolved stars (e.g., luminosity classes III and II). Thus, considering only the sample actually observed in the BCD system, which encompasses $N_{\rm tot}$ = 198 B + Be + Bdd stars (luminosity classes from ZAMS to bright giants) of which $N_{\rm e}$ = 42 are Be stars, we obtain $f = N_{\rm e}/N_{\rm tot}$ = 21%. This percentage is higher than that reported by Zorec & Briot (1997) for the field of galactic Be stars (∼17%). While among the 13 (∼7%), 11 are dwarfs and 2 are giants. Table 7 lists the Be and Bdd stars used for this analysis.

We notice that according to the weather conditions, several observing restrictions and other stellar sample selections, the above fraction f = 21% of B emission-line stars can be biased, mainly because part of the sample of Be stars were not selected randomly. In order to evaluate a possible overestimate of the actual fraction of Be stars that we calculated for open clusters, we first compared this fraction with the fraction that can be derived using the available Be and B stars in the WEBDA database for the same 11 clusters. Thus, in the WEBDA database we counted 57 Be stars among 236 B stars. This implies 24%, which is a higher percentage than we estimated for Be stars in this work. However, we must keep in mind that not all stars in the WEBDA database are necessarily cluster members.

A second test is to compute a Monte Carlo simulation of the distribution of an "actual" fraction, $f_{\rm actual}$ = 21% B emission-line stars for $N_{\rm tot}$ = 198 B + Be + Bdd stars in 11 open clusters, over 100 independent samplings. We obtained thus an average $\langle f_{\rm simulated}\rangle$ = 22% B emission-line stars with dispersion $\sigma_{\rm f}$ = 9%. If we had observed $N_{\rm tot}$ = 2000 B + Be + Bdd stars,

Table 7. Be and Bdd stars belonging to open clusters.

ID	ST	Group	Paper reference
Cr 223 021[dd]	A1V	Bdd	II
Cr 223 106[dd]	B5IV	Bdd	II
HD 305 296[dd]	B0Ve	Be	II
Hogg 16a 68[dd]	B4Ve	Be	II
Hogg 16b 02	B2II	Be	II
Hogg 16b 03[dd]	B1IIIe	Be	II
NGC 2645 03	B0II	Be	II
NGC 2645 04	B0IIe	Be	II
NGC 2645 05	B1IVe	Be	II
NGC 3114 003[dd]	B6IIIe	Be	II
NGC 3114 004[dd]	B8IIIe	Be	II
NGC 3114 006[dd]	B8IV	Bdd	II
NGC 3114 011[dd]	B8IV	Bdd	II
NGC 3114 028[dd]	B6IVe	Be	II
NGC 3114 033[dd]	B5IVe	Be	II
NGC 3114 079[dd]	A1V	Bdd	II
NGC 3114 091[dd]	B8IVe	Be	II
NGC 3114 129	B8Ve	Be	II
NGC 3114 132[dd]	B7:VI:	Bdd	II
NGC 3766 001	B5III	Be	I
NGC 3766 015	B4III	Be	I
NGC 3766 026	B2IVe	Be	I
NGC 3766 027	B3III	Be	I
NGC 3766 151	B3Ve	Be	I
NGC 3766 239	B3IV	Be	I
NGC 3766 240[dd]	B5IIe	Be	I
NGC 3766 264[dd]	B2Ve	Be	I
NGC 3766 291	B3Ve	Be	I
NGC 3766 301	B3Ve	Be	I
HD 308 852[dd]	B5IVe	Be	I
NGC 4755 008	B3V	Be	I
NGC 4755 011	B6V	Be	I
NGC 4755 117	B3V	Be	I
NGC 4755 202	B2IV	Be	I
NGC 4755 306[dd]	B0IIIe	Be	I
NGC 6025 01	B0Ve:	Be	II
NGC 6025 03[dd]	B5III	Bdd	II
NGC 6025 06	B6V	Be	II
NGC 6025 25[dd]	B7V	Bdd	II
NGC 6087 007[dd]	B6Ve	Be	III
NGC 6087 009[dd]	B6Ve	Be	III
NGC 6087 010[dd]	B5IIIe	Be	III
NGC 6087 011[dd]	B4V	Bdd	III
NGC 6087 014[dd]	B8V	Be	III
NGC 6087 022	B2IVe	Be	III
NGC 6087 101[dd]	A1:VI:	Bdd	III
NGC 6087 156[dd]	B6:V:	Bdd	III
NGC 6250 01[dd]	B0III	Bdd	III
NGC 6250 35	B0IVe	Be	III
NGC 6383 001	O7V	Be	III
NGC 6383 057[dd]	A2V	Bdd	III
NGC 6383 076	B3Ve	Be	III
NGC 6530 042	B0IV	Be	III
NGC 6530 065[dd]	O	Be	III
NGC 6530 100	B2VI	Be	III

Notes. [(dd)] Star with a SBD.

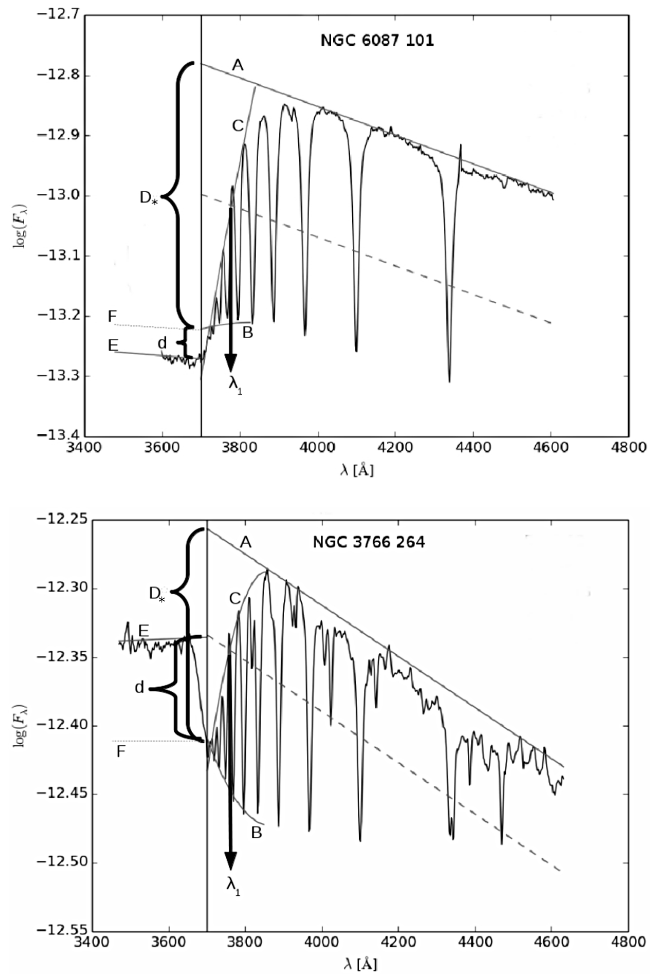

Fig. 11. Stars with a second Balmer discontinuity. The value D_* is the height of the photospheric component of the Balmer discontinuity and d is the height of the second component. In the *upper panel*, d is in absorption (Be-shell phase) and in the *lower panel* is in emission (Be phase).

the simulation predicts that we should have $\langle f_{\rm simulated} \rangle = 22\%$ B emission-line stars with $\sigma_{\rm f} = 4\%$. In this simulation we assumed that all clusters have the same age, so that each can be able to bear the same fraction of B emission-line stars. Considering differences in cluster ages, the bias $\sigma_{\rm f}$ could perhaps be larger.

Hence, both results suggest that the fraction of Be stars in open clusters is probably larger than that of field Be stars.

The spectra of the 13 Bdd stars are shown in Fig. 12 together with the spectra of the 17 Be stars with a SBD. Moreover, we have high-resolution spectra of only 7 Bdd stars in the region of Hα. With the exception of NGC 3114 11, which shows a typical shell profile, the rest of the stars display an absorption Hα line (see Fig. 13) that might be partially filled in by emission. However, as these spectra were not taken simultaneously with the spectrophotometric BCD observations, either the emission or shell features, if these features existed, could have disappeared in the meantime.

5.4. Diagram of $T_{\rm eff} - \log g$

In Fig. 14 we present a $T_{\rm eff} - \log g$ diagram derived with the BCD parameters, where we can observe that most of the B and Be stars are dwarfs ($3.5 \lesssim \log g \lesssim 4.5$) and are distributed in the whole temperature interval. A smaller number of B and

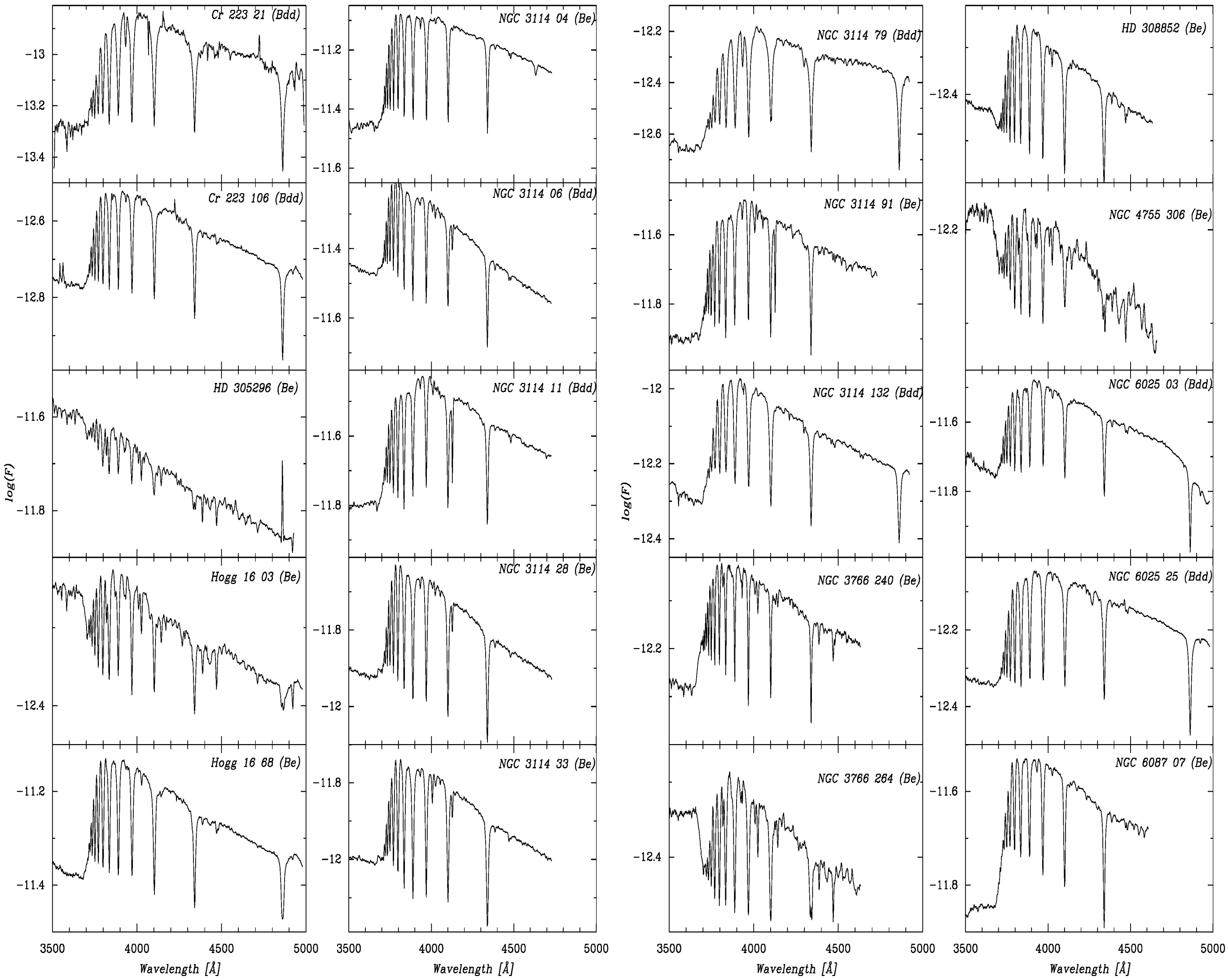

Fig. 12. Low-resolution spectra of stars with a SBD.

Be giants also seem to be uniformly distributed in the same $T_{\rm eff}$ range. This supports the results found by Mermilliod (1982); Slettebak (1985); Zorec et al. (2005) who state that Be stars occupy the whole main sequence band and the Be phenomenon occurs in very different evolutionary states. On the other hand, the sample of Bdd stars is mainly constituted by cool B dwarfs with circumstellar envelopes, as shown in next section.

5.5. Distribution of stars per spectral subtype and age

It has to be emphasized that our sampling is not complete due to the observing conditions (short running campaigns or full moon nights) that introduced strong selection effects, since sometimes we could only observe the brightest members of each clusters. However, we were able to observe almost all of the previously reported Be stars. Notwithstanding the small sample size and risk of bias in the included trials, it is still possible to discuss age-dependence trends related to the appearance of the Be phenomenon, as was previously suggested by Mathew et al. (2008); Zorec et al. (2005); Fabregat & Torrejón (2000), and to compare these trends with the presence of the new group of Bdd stars. To this purpose, we classified our sample into three age groups. The first group comprises open clusters with ages between 3 Myr and 10 Myr, the second is related to intermediate-age clusters (10−40 Myr), and the last group encompasses clusters older than 40 Myr.

For each age group we calculated the relative frequency of various kinds of stars: B, Be, and Bdd, per interval of spectral subtype. To avoid skewing the results we searched for optimal bin number and bin size per spectral subtype. Hence, we adopted a bin-width optimization method that minimized the integrated squared error (Shimazaki & Shinomoto 2007). We obtained a total of 6 bins that correspond to the spectral intervals: B0-B2, B2-B4, B4-B6, B6-B8, B8-A0, and A0-A2. The corresponding bar-graph histograms per spectral subtype and per age group are illustrated in Fig. 15, where the blue, red, and green bars represent, respectively, the relative frequency of normal B, Be, and Bdd stars within each bin.

In the plots we observe that young and intermediate-age clusters are composed of Be stars of mostly B2-B4 spectral types

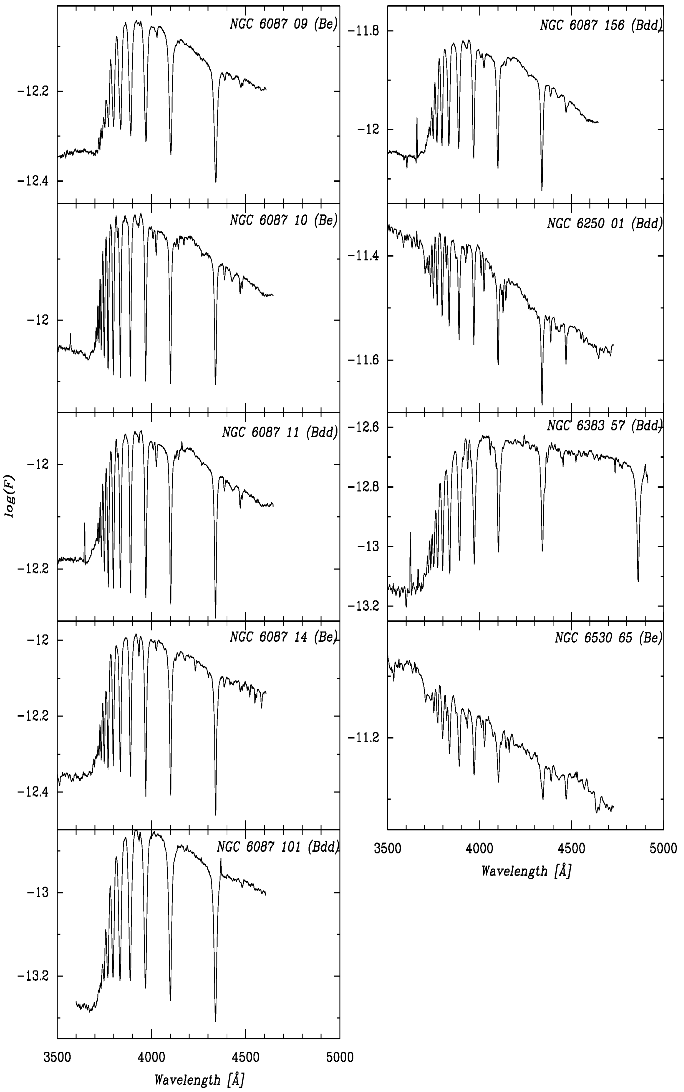

Fig. 12. continued.

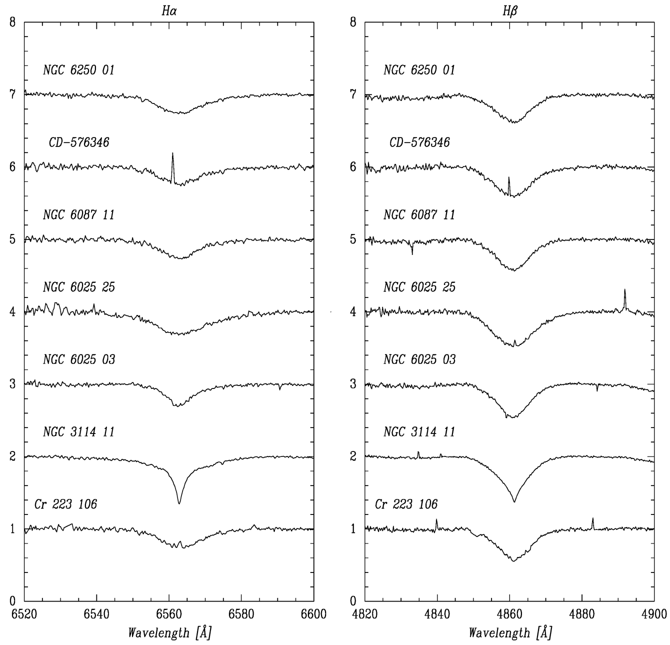

Fig. 13. Bdd Hα (*first column*) and Hβ (*second column*) profile lines.

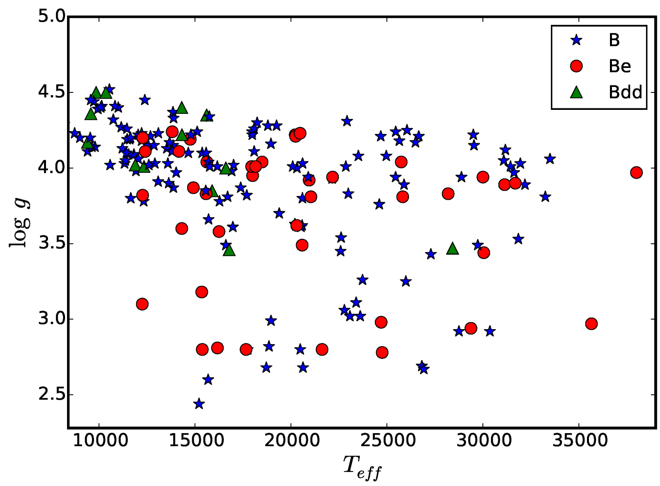

Fig. 14. Cluster star members in $T_{\rm eff}$ against $\log g$ plot. Be stars are distributed in the whole temperature interval.

and only a few Bdd stars were detected (Figs. 15a and b). We have a fraction of about 19% of Be stars in young open clusters (<10 Myr). This number then increases to about a 28% for the intermediate-age group (with ages between 10−40 Myr, see Fig. 15b) where we have the maximum Be star fraction, supporting thus previous results found by Malchenko (2008) and Fabregat & Torrejón (2000). In the intermediate-age group we also found a great number of evolved Be stars with luminosity III-II. Furthermore, in the same plot, we can observe a small fraction of Be stars at the B4-B6 types. Then, the percentage of Be stars seems to decrease in the old open clusters (∼17%, Fig. 15c), as was stressed by Mermilliod (1982) and Grebel (1997). In these old clusters, the Be phenomenon is dominated by stars with spectral types later than B4 and the maximum frequency of Be stars is around the B6-B8 types. This result indicates a clear trend of the appearance of the Be phenomenon with age.

On the other hand, if we focus on the relative frequency of Bdd stars (stars with circumstellar envelopes that are out off an emission phase) per spectral subtype (Fig. 15c), a significant number (∼12%) of Bdd stars later than B5 are present and their distribution seems to follow the frequency distribution of B and "active" Be stars. Therefore, the distribution of Bdd stars seems to complete, in number, the lack of late "active" Be stars. We interpret the result in the same sense as the hypothesis in Zorec et al. (2003), which states that the strong deficiency of the field Be stars cooler than B7 perhaps could be taken on by Bn stars (i.e., B stars with broad absorption lines). Zorec et al. (2003) also proposed that the absence of late Be stars and the increment of Bn stars is mainly because their low effective temperatures are not able to keep their circumstellar envelopes completely ionized. Thus, Bn stars could be latent Be and Be-shell stars (Zorec et al. 2003; Ghosh et al. 1999). Therefore, it would be necessary to study in more detail the properties of the Bn star population and a possible link with the Bdd star group, if they are not the same population.

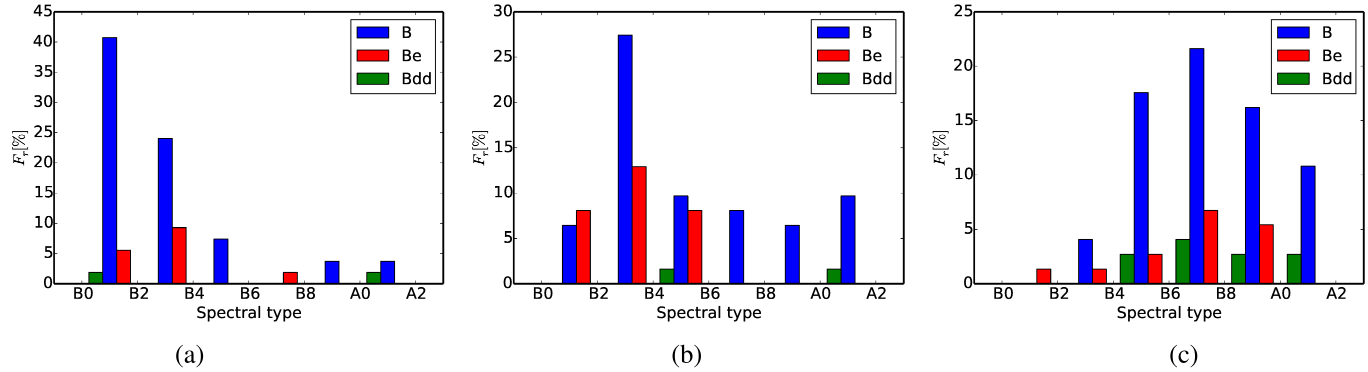

Fig. 15. Number and frequency of stars with and without circumstellar envelopes per spectral subtype in open clusters with different ages: *a*) between 3 Myr and 10 Myr, *b*) between 10 Myr and 40 Myr, and *c*) older than 40 Myr. The plots show a clear trend of the appearance of the Be phenomenon with age.

In summary, the Be phenomenon is observed in both dwarf and giant stars along the whole main sequence. In addition we confirm the trend of an age evolution of the Be phenomenon, since among the massive stars the Be phenomenon seems to appear on average at an earlier age than in the less massive stars. This result confirms previous age-dependence trends found by Mathew et al. (2008); Zorec et al. (2005); Fabregat & Torrejón (2000). In addition, we found that the number of stars with circumstellar envelopes (active and passive B emission stars) in the old age cluster group amounts to 29%, suggesting that Bdd stars might be the coldest counterpart of stars with the Be phenomenon.

From a theoretical point of view, the age evolution of the Be phenomenon was supported by Ekström et al. (2008). These authors showed that the age dependence of the Be phenomenon could be related to the increase of the ratio $V \sin i/V_{\rm crit}$ due to a lowering of $V_{\rm crit}$ (critical rotation velocity) of stars with age via the transport of angular momentum by meridional circulation to the surface and stellar wind of the star. On the other hand, the rotation modifies stellar pulsations, since centrifugal force distorts the resonant cavity of the pulsations and the Coriolis force modifies the dynamic of the modes (Ouazzani et al. 2012). As well, the evolutionary changes affect the pulsational properties of the stars due to changes in the gravity and the isentropic sound velocity and density (Bruggen & Smeyers 1987). Therefore, both rotation and pulsation modes might compete to release material from the star to fill a disk. Therefore, our knowledge about the evolution effects of rotation and pulsational modes, and their interplay, is crucial to understand the mechanism of ejection of mass and disk formation.

6. Conclusions

In this work we used the BCD spectrophotometric system, based on measurable quantities of the stellar continuum spectrum around the BD, to directly determine the fundamental parameters (spectral type, luminosity class, $T_{\rm eff}$, $\log g$, $M_{\rm v}$, $M_{\rm bol}$, and $\Phi_{\rm b}^0$) of 68 B and Be stars in four open clusters. In addition, we were able to derive individual values of the stellar distance modulus, color excess $E(B-V)$, luminosity, mass, and age for the whole sample. From these measurements we obtained the cluster parameters.

Thus, this work completes the study of the determination of cluster parameters for 11 open clusters (Collinder 223, Hogg 16, NGC 2645, NGC 3114, NGC 3766, NGC 4755, NGC 6025, NGC 6087, NGC 6250, NGC 6383, and NGC 6530), which are summarized in Table 8. Particularly, the distance determinations obtained through the BCD method for NGC 2645, NGC 6087, NGC 6250, and NGC 6383 agree with distance estimates obtained with classical photometric methods.

Table 8. Open cluster parameters derived with the BCD method.

Open cluster	$E(B-V)$ [mag]	$(m_{\rm v}-M_{\rm v})_0$ [mag]	Age [Myr]
Collinder 223	0.25 ± 0.03	11.21 ± 0.25	~25
Hogg 16a	0.26 ± 0.03	8.91 ± 0.26	<40
Hogg 16b	0.65 ± 0.09	12.78 ± 0.32	10–16
NGC 2645	0.54 ± 0.07	12.39 ± 0.30	6–14
NGC 3114	0.05 ± 0.01	9.21 ± 0.15	~100
NGC 3766	0.25 ± 0.02	11.50 ± 0.15	6–28
NGC 4755	0.30 ± 0.04	12.10 ± 0.22	~8
NGC 6025	0.34 ± 0.02	9.25 ± 0.17	40–68
NGC 6087	0.35 ± 0.03	9.00 ± 0.19	~55
NGC 6250	0.38 ± 0.16	10.55 ± 0.33	6
NGC 6383	0.51 ± 0.03	9.61 ± 0.38	3–10
NGC 6530	0.26 ± 0.05	11.76 ± 0.20	4–6

In addition, from our whole spectroscopic study, we find 6 new Be stars and 15 late B stars with circumstellar envelopes out of an emission phase (Bdd stars). The Be star population represents 21% of the sample of cluster stars, which is larger than the current population of field Be stars (17%), while the Bdd star group represents ~1/3 of the Be star population.

We also identify four blue straggler candidates: HD 305 296 (in Collinder 223), NGC 6025 12, NGC 6087 12, and NGC 6530 7.

The maximum distribution of Be stars per spectral subtype presents a maximum at the B2-B4 spectral type in young and intermediate-age open clusters whereas this maximum is at the B6-B8 type in the old clusters. In addition, we find that ~30% of the cluster B stars have circumstellar envelopes (Be + Bdd stars).

Finally, our result supports the statement that the Be phenomenon occurs in very different evolutionary states and occupies the whole main sequence band. On the other hand, we find a clear indication of an increase with age of the fraction of stars showing the Be phenomenon, which is confirmed by the increase of the fraction number of Be stars at the spectral types B2-B4 in the age interval 10−40 Myr. In old open clusters we found a great number of low massive (later than B4) stars with circumstellar envelopes, although they did not have detectable emission-line signatures (Bdd stars). This last group was detected because of the presence of a second BD.

Acknowledgements. We would like to thank our anonymous referee for a careful reading and valuable comments and suggestions that certainly helped to improve this manuscript. YJA: Visiting Astronomer, Complejo Astronómico El Leoncito operated under agreement between the Consejo Nacional de Investigaciones Científicas y Técnicas de la República Argentina and the National Universities of La Plata, Córdoba and San Juan. This research has made use of the SIMBAD database, operated at CDS, Strasbourg, France, and WEBDA database, operated at the Department of Theoretical Physics and Astrophysics of the Masaryk University. This work was granted by the National University of La Plata (jóvenes investigadores 2016). L.C. appreciates financial support from CONICET (PIP 0177) and the Universidad Nacional de La Plata (Programa de Incentivos G11/137), Argentina.

References

Aidelman, Y. J., Cidale, L. S., Zorec, J., & Arias, M. L. 2010, Boletin de la Asociacion Argentina de Astronomia, 53, 141
Aidelman, Y., Cidale, L. S., Zorec, J., & Arias, M. L. 2012, A&A, 544, A64
Aidelman, Y., Cidale, L. S., Zorec, J., & Panei, J. A. 2015, A&A, 577, A45
An, D., Terndrup, D. M., & Pinsonneault, M. H. 2007, ApJ, 671, 1640
Antalová, A. 1972, Bulletin of the Astronomical Institutes of Czechoslovakia, 23, 126
Barbier, D., & Chalonge, D. 1939, ApJ, 90, 627
Battinelli, P., & Capuzzo-Dolcetta, R. 1991, MNRAS, 249, 76
Baumgardt, H., Dettbarn, C., & Wielen, R. 2000, A&AS, 146, 251
Becker, W., & Fenkart, R. 1971, A&AS, 4, 241
Boehm-Vitense, E., Hodge, P., & Boggs, D. 1984, ApJ, 287, 825
Boggs, D., & Bohm-Vitense, E. 1989, ApJ, 339, 209
Breger, M. 1966, PASP, 78, 293
Bruggen, P., & Smeyers, P. 1987, A&A, 186, 170
Chalonge, D., & Divan, L. 1973, A&A, 23, 69
Chini, R., & Neckel, T. 1981, A&A, 102, 171
Cidale, L., Zorec, J., & Tringaniello, L. 2001, A&A, 368, 160
Cidale, L. S., Arias, M. L., Torres, A. F., et al. 2007, A&A, 468, 263
Clariá, J. J., & Lapasset, E. 1991, PASP, 103, 998
Cochetti, Y. R., Arias, M. L., Cidale, L., & Zorec, J. 2013, Boletin de la Asociacion Argentina de Astronomia, 56, 207
Cochetti, Y. R., Arias, M. L., Cidale, L. S., Granada, A., & Zorec, J. 2015, Boletin de la Asociacion Argentina de Astronomia, 57, 108
Cook, K. H., Alcock, C., Allsman, H. A., et al. 1995, in Astrophysical Applications of Stellar Pulsation, eds. R. S. Stobie & P. A. Whitelock, IAU Colloq. 155 (Springer), ASP Conf. Ser., 83, 221
Cox, A. N. 2000, Allen's astrophysical quantities (New York: AIP Press)
De Loore, C., Hensberge, H., Sterken, C., et al. 1979, A&A, 78, 287
de Wit, W. J., Lamers, H. J. G. L. M., Marquette, J. B., & Beaulieu, J. P. 2006, A&A, 456, 1027
Dias, W. S., Alessi, B. S., Moitinho, A., & Lépine, J. R. D. 2002, A&A, 389, 871
Dias, W. S., Monteiro, H., Caetano, T. C., et al. 2014, A&A, 564, A79
Didelon, P. 1982, A&AS, 50, 199
Divan, L. 1979, in Ricerche Astronomiche, Vol. 9, Spectral Classification of the Future, eds. M. F. McCarthy, A. G. D. Philip, & G. V. Coyne, IAU Colloq. 47, 247
Divan, L., & Zorec, J. 1982, in Be Stars, eds. M. Jaschek, & H.-G. Groth, IAU Symp., 98, 61
Divan, L., Zorec, J., & Andrillat, Y. 1983, A&A, 126, L8
Dufton, P. L., Smartt, S. J., Lee, J. K., et al. 2006, A&A, 457, 265
Eggen, O. J. 1961, Royal Greenwich Observatory Bulletins, 27, 61
Ekström, S., Meynet, G., Maeder, A., & Barblan, F. 2008, A&A, 478, 467
Ekström, S., Georgy, C., Eggenberger, P., et al. 2012, A&A, 537, A146
Fabregat, J., & Torrejón, J. M. 2000, A&A, 357, 451
Feast, M. W. 1957, MNRAS, 117, 193
Feinstein, A. 1994, Rev. Mex. Astron. Astrofis., 29, 141
Feinstein, C., Vergne, M. M., Martínez, R., & Orsatti, A. M. 2008, MNRAS, 391, 447
Fernie, J. D. 1961, ApJ, 133, 64
Fitzgerald, M. P., Jackson, P. D., Luiken, M., Grayzeck, E. J., & Moffat, A. F. J. 1978, MNRAS, 182, 607
Fitzgerald, M. P., Boudreault, R., Fich, M., Luiken, M., & Witt, A. N. 1979a, A&AS, 37, 351
Fitzgerald, M. P., Luiken, M., Maitzen, H. M., & Moffat, A. F. J. 1979b, A&AS, 37, 345
Frémat, Y., Zorec, J., Hubert, A., & Floquet, M. 2005, A&A, 440, 305
Gerbaldi, M., & Zorec, J. 1993, in Inside the Stars, eds. W. W. Weiss, & A. Baglin, IAU Colloq. 137, ASP Conf. Ser., 40, 150
Ghosh, K. K., Apparao, K. M. V., & Pukalenthi, S. 1999, A&AS, 134, 359
Gkouvelis, L., Fabregat, J., Zorec, J., et al. 2016, A&A, 591, A140
Graham, J. A. 1967, MNRAS, 135, 377
Grebel, E. K. 1997, A&A, 317, 448
Harris, G. L. H. 1976, ApJS, 30, 451
Herbst, W. 1977, AJ, 82, 902
Hiltner, W. A., Morgan, W. W., & Neff, J. S. 1965, ApJ, 141, 183
Hubert, A. M., & Floquet, M. 1998, A&A, 335, 565
Hubert, A. M., Floquet, M., & Zorec, J. 2000, in The Be Phenomenon in Early-Type Stars, eds. M. A. Smith, H. F. Henrichs, & J. Fabregat, IAU Colloq. 175, ASP Conf. Ser., 214, 348
Janes, K., & Adler, D. 1982, ApJS, 49, 425
Johnson, H. L., Hoag, A. A., Iriarte, B., Mitchell, R. I., & Hallam, K. L. 1961, Lowell Observatory Bulletin, 5, 133
Keller, S. C., Bessell, M. S., Cook, K. H., Geha, M., & Syphers, D. 2002, AJ, 124, 2039
Kharchenko, N. V., Piskunov, A. E., Röser, S., Schilbach, E., & Scholz, R.-D. 2005, A&A, 438, 1163
Kharchenko, N. V., Berczik, P., Petrov, M. I., et al. 2009, A&A, 495, 807
Kharchenko, N. V., Piskunov, A. E., Schilbach, E., Röser, S., & Scholz, R.-D. 2013, A&A, 558, A53
Kilambi, G. C. 1975, PASP, 87, 975
Kilambi, G. C. 1977, MNRAS, 178, 423
Kumar, B., Sagar, R., Sanwal, B. B., & Bessell, M. S. 2004, MNRAS, 353, 991
Landolt, A. U. 1963, AJ, 68, 283
Landolt, A. U. 1964, ApJS, 8, 329
Landstreet, J. D., Silaj, J., Andretta, V., et al. 2008, A&A, 481, 465
Lindoff, U. 1968, Arkiv for Astronomi, 5, 1
Lloyd Evans, T. 1978, MNRAS, 184, 661
Lodén, L. O., & Nordström, B. 1969, Arkiv for Astronomi, 5, 231
Loktin, A. V., & Beshenov, G. V. 2001, Astron. Lett., 27, 386
Maitzen, H. M. 1985, A&AS, 62, 129
Malchenko, S. L. 2008, Odessa Astronomical Publications, 21, 60
Martin, A. J., Stift, M. J., Fossati, L., et al. 2017, MNRAS, 466, 613
Martins, F., Schaerer, D., & Hillier, D. J. 2005, A&A, 436, 1049
Mathew, B., Subramaniam, A., & Bhatt, B. C. 2008, MNRAS, 388, 1879
Mayne, N. J., & Naylor, T. 2008, MNRAS, 386, 261
McSwain, M. V., & Gies, D. R. 2005, ApJS, 161, 118
McSwain, M. V., Huang, W., Gies, D. R., Grundstrom, E. D., & Townsend, R. H. D. 2008, ApJ, 672, 590
McSwain, M. V., Huang, W., & Gies, D. R. 2009, ApJ, 700, 1216
Mennickent, R. E., Pietrzyński, G., Gieren, W., & Szewczyk, O. 2002, A&A, 393, 887
Mermilliod, J. C. 1982, A&A, 109, 48
Meynet, G., Mermilliod, J.-C., & Maeder, A. 1993, A&AS, 98, 477
Moffat, A. F. J., & Vogt, N. 1975, A&AS, 20, 155
Moujtahid, A., Zorec, J., Hubert, A. M., Garcia, A., & Burki, G. 1998, A&AS, 129, 289
Moujtahid, A., Zorec, J., & Hubert, A. M. 1999, A&A, 349, 151
Niedzielski, A., & Muciek, M. 1988, Acta Astron., 38, 225
Ouazzani, R.-M., Dupret, M.-A., & Reese, D. R. 2012, A&A, 547, A75
Pandey, A. K., Bhatt, B. C., Mahra, H. S., & Sagar, R. 1989, MNRAS, 236, 263
Paunzen, E., Netopil, M., & Zwintz, K. 2007, A&A, 462, 157
Penston, M. V. 1964, The Observatory, 84, 141
Piskunov, A. E. 1980, Bulletin d'Information du Centre de Donneés Stellaires, 19, 67
Piskunov, A. E., Schilbach, E., Kharchenko, N. V., Röser, S., & Scholz, R.-D. 2007, A&A, 468, 151
Piskunov, A. E., Schilbach, E., Kharchenko, N. V., Röser, S., & Scholz, R.-D. 2008, A&A, 477, 165
Prisinzano, L., Damiani, F., Micela, G., & Sciortino, S. 2005, A&A, 430, 941
Rastorguev, A. S., Glushkova, E. V., Dambis, A. K., & Zabolotskikh, M. V. 1999, Astron. Lett., 25, 595
Rauw, G., & De Becker, M. 2008, in The Multiwavelength Picture of Star Formation in the Very Young Open Cluster NGC 6383, ed. B. Reipurth, 497
Robichon, N., Arenou, F., Mermilliod, J.-C., & Turon, C. 1999, A&A, 345, 471
Sagar, R. 1987, MNRAS, 228, 483
Sagar, R., & Cannon, R. D. 1997, A&AS, 122, 9
Sagar, R., & Joshi, U. C. 1978, MNRAS, 184, 467

Sagar, R., Piskunov, A. E., Miakutin, V. I., & Joshi, U. C. 1986, MNRAS, 220, 383
Sahade, J., & Berón Dàvila, F. 1963, Annales d'Astrophysique, 26, 153
Sanford, R. F. 1949, ApJ, 110, 117
Schmidt, E. G. 1980, AJ, 85, 158
Shimazaki, H., & Shinomoto, S. 2007, Neural Computation, 19, 1503
Shobbrook, R. R. 1985, MNRAS, 212, 591
Slettebak, A. 1985, ApJS, 59, 769
Sota, A., Maíz Apellániz, J., Walborn, N. R., et al. 2011, ApJS, 193, 24
Strobel, A., Skaba, W., & Proga, D. 1992, A&AS, 93, 271
Sung, H., Chun, M.-Y., & Bessell, M. S. 2000, AJ, 120, 333
The, P.-S. 1965, Contributions from the Bosscha Observervatory, 32, 0
The, P.-S. 1966, Contributions from the Bosscha Observervatory, 34, 1
The, P. S., Hageman, T., Tjin A Djie, H. R. E., & Westerlund, B. E. 1985, A&A, 151, 391
Torres, A. V. 1987, ApJ, 322, 949
Tosi, M. 1979, Mem. Soc. Astron. It., 50, 245
Trumpler, R. J. 1930, Lick Observatory Bulletin, 14, 154
Turner, D. G. 1986, AJ, 92, 111
van Altena, W. F. 1972, ApJ, 178, L127
van den Ancker, M. E., The, P. S., Feinstein, A., et al. 1997, A&AS, 123, 63
van den Ancker, M. E., Thé, P. S., & de Winter, D. 2000, A&A, 362, 580
Vinicius, M. M. F., Zorec, J., Leister, N. V., & Levenhagen, R. S. 2006, A&A, 446, 643
Walker, M. F. 1957, ApJ, 125, 636
Wright, E. L., Eisenhardt, P. R. M., Mainzer, A. K., et al. 2010, AJ, 140, 1868
Zhao, J.-L., Chen, L., & Wen, W. 2006, Chin. J. Astron. Astrophys., 6, 435
Zorec, J. 1986, Thèse d'État, Université Paris VII
Zorec, J., & Briot, D. 1991, A&A, 245, 150
Zorec, J., & Briot, D. 1997, A&A, 318, 443
Zorec, J., Divan, L., & Hoeflich, P. 1989, A&A, 210, 279
Zorec, J., Frémat, Y., Cidale, L. S., Chauville, J., & Ballereau, D. 2003, Boletin de la Asociacion Argentina de Astronomia, 46, 30
Zorec, J., Frémat, Y., & Cidale, L. 2005, A&A, 441, 235
Zorec, J., Cidale, L., Arias, M. L., et al. 2009, A&A, 501, 297
Zorec, J., Frémat, Y., Domiciano de Souza, A., et al. 2016, A&A, 595, A132
Zug, R. S. 1937, Lick Observatory Bulletin, 18, 89